Mon. Not. R. Astron. Soc. **000**, 1–26 (2000) Printed 1 February 2008 (MN LATEX style file v1.4)

Direct N-body Modelling of Stellar Populations: Blue Stragglers in M67

Jarrod R. Hurley[1,3], Christopher A. Tout[1], Sverre J. Aarseth[1] and Onno R. Pols[2]
[1] *Institute of Astronomy, Madingley Road, Cambridge CB3 0HA, UK*
[2] *Department of Mathematics, P.O. Box 28M, Monash University, Victoria, 3800, Australia*
[3] *Current address: Department of Astrophysics, American Museum of Natural History, Central Park West at 79th Street, New York, NY 10024*
E-mail: jhurley@amnh.org, cat@ast.cam.ac.uk, sverre@ast.cam.ac.uk, onno@mail.maths.monash.edu.au

arXiv:astro-ph/0012113v1 5 Dec 2000

1 February 2008

ABSTRACT
We present a state-of-the-art N-body code which includes a detailed treatment of stellar and binary evolution as well as the cluster dynamics. This code is ideal for investigating all aspects relating to the evolution of star clusters and their stellar populations. It is applicable to open and globular clusters of any age. We use the N-body code to model the blue straggler population of the old open cluster M67. Preliminary calculations with our binary population synthesis code show that binary evolution alone cannot explain the observed numbers or properties of the blue stragglers. On the other hand, our N-body model of M67 generates the required number of blue stragglers and provides formation paths for all the various types found in M67. This demonstrates the effectiveness of the cluster environment in modifying the nature of the stars it contains and highlights the importance of combining dynamics with stellar evolution. We also perform a series of $N = 10\,000$ simulations in order to quantify the rate of escape of stars from a cluster subject to the Galactic tidal field.

Key words: methods: numerical – stars: evolution – stars: blue stragglers – binaries: general – globular clusters: general – open clusters and associations: M67

1 INTRODUCTION

The rich environment of a star cluster provides an ideal laboratory for the study of self-gravitating systems. It also provides important tests for stellar evolution theory and the formation of exotic stars and binaries. The colour-magnitude diagram (CMD) is convenient for displaying the range of photometrically observable stellar populations within a star cluster. However, in the case of dense or dynamically old clusters, the appearance of the CMD can be significantly altered by dynamical encounters between the cluster stars. Therefore it is necessary to combine population synthesis with a description of the cluster dynamics. This is important for both gravitational and non-gravitational interactions between stars as well as the dynamical evolution of the cluster as a whole. Our approach in this area is to include a consistent treatment of stellar and binary evolution in a state-of-the-art N-body code so as to allow the generation and interaction of the full range of stellar populations within a cluster environment (Hurley et al. 2000). The stellar evolution algorithm that we use includes variable metallicity which enables us to produce realistic cluster models for comparison with observed cluster populations of any age. As the first group to have this capability we are now embarking on a major project to investigate the dynamical evolution of star clusters and their populations.

Blue stragglers are cluster main-sequence (MS) stars that seem to have stayed on the main-sequence for a time exceeding that expected from standard stellar evolution theory for their mass: they lie above and blueward of the turn-off in a cluster CMD. Ahumada & Lapasset (1995) conducted an extensive survey of blue straggler candidates in Galactic open clusters. Their results are plotted in Figure 1 as the mean number of blue stragglers per open cluster, relative to the number of main-sequence stars in the two magnitudes below the turn-off, as a function of the cluster age. Also shown in Figure 1 is the point for the old open cluster M67 (NGC 2682) which stands out above the mean for its age, containing 29 proposed blue stragglers with high probability of cluster membership.

Milone & Latham (1992a, hereinafter ML) have undertaken a long-term radial velocity observational program to study the blue stragglers of M67. Of a total of ten well-observed blue stragglers they find that six are members of spectroscopic binaries. One of these is a short-period binary; F190 with a period of 4.183 d and an eccentricity of 0.205 (Milone & Latham 1992b). The others are long-period binaries with periods from 846 to 4913 d; three have eccentric

© 2000 RAS

orbits and two have orbits consistent with being circular (Latham & Milone 1996). Thus, if the ML sample is taken as representative of the overall M67 blue straggler population, then for every ten blue stragglers we expect four to be single stars and six to be found in binaries with about two of these circular and at least four eccentric.

This raises the question of how the blue stragglers formed with the most obvious scenarios involving binary evolution. A Case A mass transfer scenario (Kippenhahn, Weigert & Hoffmeister 1967) involves a main-sequence star filling its Roche-lobe and transferring mass to its companion, a less massive main-sequence star, followed by coalescence of the two stars as the orbit shrinks owing to angular momentum loss. The result is a more massive main-sequence star that is rejuvenated relative to other stars of the same mass and thus evolves to become a blue straggler. This is an efficient method of producing single blue stragglers provided that a large population of close binaries exists in the cluster. Case B mass transfer involves a main-sequence star accreting material from a more evolved companion and thus could be a likely explanation for blue stragglers in short-period spectroscopic binaries, such as F190. Blue stragglers in long-period binaries could be produced by Case C mass transfer when the primary is an asymptotic giant branch (AGB) star that has lost much of its mass. Wind accretion in binaries that initially have fairly large periods could also be responsible for such systems.

In all these cases, except perhaps wind accretion, the binary orbits should be circularized by tides before and during mass transfer. Other scenarios are needed to explain the binaries in eccentric orbits and this is where the effects of dynamical interactions in a cluster environment become important. Physical stellar collisions during binary-binary and binary-single interactions can produce blue stragglers in eccentric orbits as well as allowing the possibility of an existing blue straggler being exchanged into an eccentric binary. According to Davies (1996) encounters between binaries and single stars become important when the binary fraction in the core exceeds about 5% and binary-binary encounters dominate if the fraction is greater than 30%. Additionally, the probability of encounters depends on the density of the cluster. It is also possible that perturbations from passing stars may induce an eccentricity in a previously circular orbit. As discussed by Leonard (1996) it is unlikely that any one formation mechanism dominates and in the case of the diverse blue straggler population of M67 it seems probable that all the above scenarios play a role.

The aim of this paper is to compare N-body models with observations of M67 to investigate the incidence and distribution of blue stragglers (BSs) and in so doing to constrain the nature of the primordial binary population. In Section 2 we give an overview of the observational data, in terms of individual stellar populations and overall cluster parameters. We describe the details of our binary population synthesis in Section 3 and use it to constrain the parameters of the various distributions involved, with a view to maximizing the number of blue stragglers produced. The N-body code is described in Section 4 and then used in Section 5 to quantify the rate of escape of stars from a cluster subject to the tidal field of our Galaxy. In Section 6 we present our N-body model of M67 paying particular attention to the evolution of the blue straggler population. Our discussion of the results is then given, followed by conclusions.

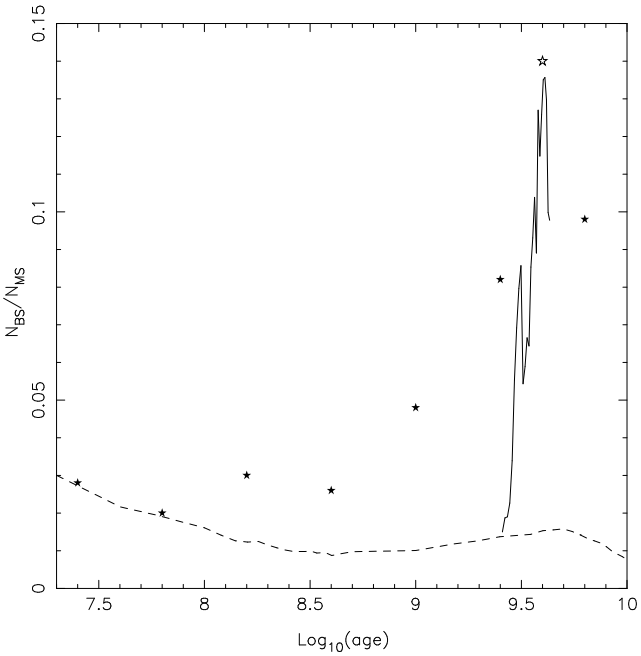

Figure 1. The number of blue stragglers relative to the number of MS stars in the two magnitudes below the turn-off as a function of the population age. The stars represent the open cluster data of Ahumada & Lapasset (1995) with the M67 point an open symbol. The dotted line represents our population synthesis with a 50% binary population using the parameters of PS6 (see Section 3). The solid line represents our M67 N-body simulation (see Section 6, note that the log-scale does not clearly indicate the length of the simulation).

2 OBSERVATIONAL DATA FOR M67

We use the CCD photometric data of Montgomery, Marschall & Janes (1993, hereinafter MMJ) taken from the Open Cluster Database (OCD: Mermilliod 1996) to construct the M67 CMD shown in Figure 2. Proper motion studies by Sanders (1977) and Girard et al. (1989) distinguish stars with membership probabilities of at least 80% from less certain members. The CMD shows a well-defined photometric binary sequence, from which MMJ find that at least 38% of the stars in the cluster are binary systems. Of the BSs identified by the OCD, according to the study of Ahumada & Lapasset (1995), eleven are obvious candidates from inspection of the CMD. These eleven are all in the ML sample which is listed in Table 1 with each star indicated by its Sanders (1977) number. The rest of the BSs are much closer to the MS and its turn-off, in a clump with $(B-V) > 0.35$ and $V > 11.8$. The two most obvious of these complete the ML sample of thirteen BSs, three of which were rotating too rapidly to allow reliable velocity determinations. Of particular interest among the sample is the super-BS F81 which is a single star and has a mass of $\simeq 3\,\mathrm{M}_\odot$ (Leonard 1996), more than a factor of 2 greater than the cluster turn-off mass, $M_{\rm TO} \simeq 1.3\,\mathrm{M}_\odot$. The binary S1072 is classified on the OCD as containing a BS but this

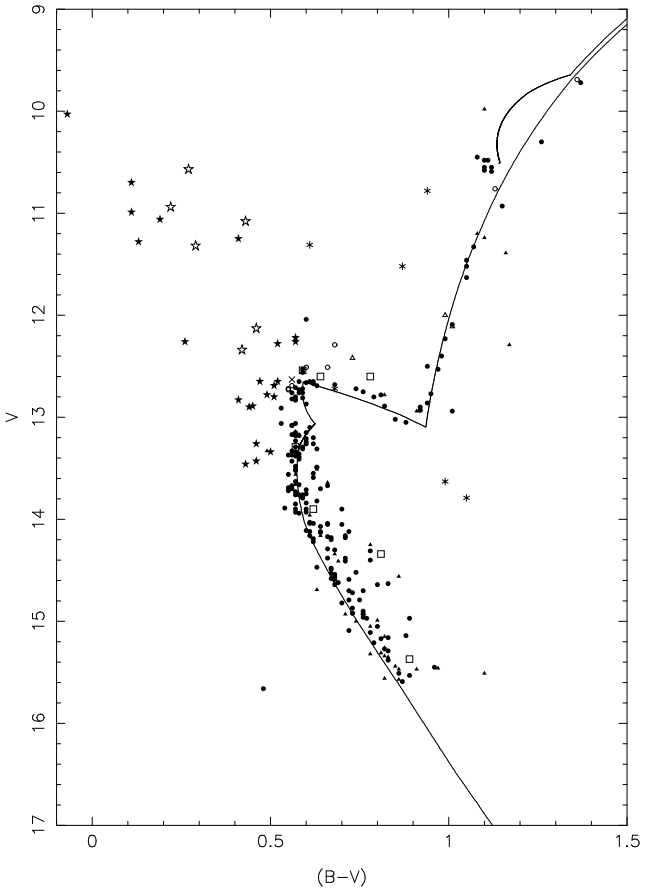

Figure 2. CMD for M67 (NGC 2682) using photometric data taken from the Open Cluster Database(OCD: Mermilliod 1996). Circles show probable members ($P_{\rm mb} \geq 80\%$) as indicated by proper motion studies and triangles show stars of less certain membership. Open symbols are spectroscopic binaries. Stars identified as blue stragglers in the OCD are plotted with stars. Open squares represent the seven RS CVn candidates identified by Belloni, Verbunt & Mathieu (1998, BVM). Asterisks are the six X-ray sources examined by van den Berg, Verbunt & Mathieu (1999, MVB), excluding S1082 which has already been plotted as a blue straggler. The cross represents the triple system observed by Mathieu, Latham & Griffin (1990, MLG). All the special stars that we have highlighted have $P_{\rm mb} \geq 80\%$. Also plotted (full line) is an isochrone at $t = 4\,160$ Myr with $Z = 0.02$, $m - M = 9.7$ and $E(B-V) = 0.015$.

is not compatible with *ubvy* photometry of the system (e.g. van den Berg, Verbunt & Mathieu 1999, hereinafter MVB) so we do not count it as a BS. This leaves 28 possible BSs of which two have membership probability less than 80% and almost 2/3 have a membership probability of 98% or greater. Half of the 26 with $P_{\rm mb} \geq 80\%$ are the BSs that have been extensively studied by ML, who found that roughly half of their sample were in binaries.

Belloni, Verbunt & Mathieu (1998, hereinafter BVM) describe the results of a ROSAT study of X-ray emission from M67. They detect 25 X-ray sources of which three are optically identified with circular binaries of orbital periods less than 10 d suggesting that they are RS Canum Venaticorum (RS CVn) stars. These three are listed in Table 1 along with four other X-ray sources that are each identified with a spectroscopic binary (SB) that has an unknown orbital solution and may possibly be RS CVn stars. Hall (1976) defined RS CVn systems to have periods between one and fourteen days, a hotter component of spectral type F-GV-IV, and strong H and K calcium lines seen in emission. The H and K emission is generally associated with the cool star which is usually a sub-giant. Multiply periodic variations in the light curves of these systems have been linked to spots on the cool star suggesting enhanced magnetic activity. This can be explained by rapid rotation of the cool primary star caused by tidal interaction with the orbit which is therefore likely to be circular. Mass-ratios have been determined for a number of eclipsing RS CVn systems (Popper 1980) and are generally close to one but in several cases are greater than one, when $q = M_2/M_1$. Here we let M_1 denote the primary mass and M_2 the secondary mass, with the primary defined as the more massive star at formation of the system. However, the primary star is not close to filling its Roche-lobe in any of these systems so the mass inversion is likely due to a slow mass exchange such as wind accretion by the secondary from the primary, or simply rapid mass loss from the primary (Tout & Eggleton 1988). X-ray sources in M67 which have not been identified with an optical counterpart by BVM are unlikely to be RS CVn systems because the presence of at least one sub-giant or giant would make them highly visible. Therefore the seven possible RS CVn systems is an upper limit to the expected number in M67.

MVB obtained optical spectra for the seven X-ray sources found by BVM for which the X-ray emission is unexplained. The parameters of these systems are also listed in Table 1. One of these sources is the BS S1082 which was determined by ML to be single. However MVB found a second component in the spectrum of this star which they interpret as a hot sub-luminous companion. Also among the sample are two so-called *subsubgiants* whose nature is not yet understood.

The metallicity given for M67 on the OCD is solar although values determined by other authors would indicate that it is slightly sub-solar, e.g. [Fe/H] $= -0.04 \pm 0.12$ (Hobbs & Thorburn 1991) and [Fe/H] $= -0.09 \pm 0.07$ (Friel & Janes 1993). The reddening of M67 is reported by various authors to be either $E(B-V) = 0.032$ (Nissen, Twarog & Crawford 1987), $E(B-V) = 0.034 \pm 0.019$ (Fan et al. 1996) or $E(B-V) = 0.05$ (MMJ), which is rather small considering its distance of about 800 pc (OCD) from the Sun. M67 is an old open cluster with an age of 4 to 5 Gyr. Carraro et al. (1994) used $Z \simeq 0.016$, a distance modulus of $m - M = 9.5$ and $E(B-V) = 0.02$ to derive an age of 4.8 Gyr with isochrones based on stellar models that included some convective overshooting. Fan et al. (1996) used a similar metallicity and distance modulus to obtain an age of 4.0 Gyr from their CCD observations of M67 while the OCD gives an age of 5.2 Gyr using $m - M = 9.75$. The detailed models of Pols et al. 1998, also including convective overshoot, used in conjunction with $Z = 0.017$, $m - M = 9.6$ and $E(B-V) = 0.032$ give an age of 4.17 Gyr. From the white dwarf cooling sequence observed in M67 Richer et al. (1998) deduce an age of 4.3 Gyr. Shown on Figure 2 is an isochrone at $t = 4.16$ Gyr computed using the stellar evolution formulae of Hurley, Pols & Tout (2000) with $Z = 0.02$, $m - M = 9.7$ and $E(B-V) = 0.015$. We convert to observed colours with bolometric corrections com-

ID #	V	$B-V$	P(d)	e	Ref.	comments
S0752	11.32	0.29	1003	0.317	ML	BS binary
S0968	11.28	0.13			ML	BS single
S0975	11.08	0.43	1221	0.088	ML	BS binary
S0977	10.03	-0.07			ML	BS single (F81)
S0997	12.13	0.46	4913	0.342	ML	BS binary
S1066	10.99	0.11			ML	BS, fast rotator
S1082	11.25	0.41			ML	BS single
S1195	12.34	0.42	1154	0.066	ML	BS binary
S1263	11.06	0.19			ML	BS single
S1267	10.57	0.27	846	0.475	ML	BS binary
S1280	12.26	0.26			ML	BS, fast rotator
S1284	10.94	0.22	4.18	0.205	ML	BS binary (F190)
S1434	10.70	0.11			ML	BS, fast rotator
S0760	13.29	0.57	-	-	BVM	SB, poss. RS CVn
S0972	15.37	0.89	-	-	BVM	SB, poss. RS CVn
S0999	12.60	0.78	10.06	0.00	BVM	RS CVn
S1019	14.34	0.81	-	-	BVM	SB, poss. RS CVn
S1045	12.54	0.59	7.65	0.00	BVM	RS CVn
S1070	13.90	0.62	2.66	0.00	BVM	RS CVn
S1077	12.60	0.64	-	-	BVM	SB, poss. RS CVn
S1040	11.52	0.87	42.83	0.027	MVB	giant + WD
S1063	13.79	1.05	18.39	0.217	MVB	subsubgiant
S1072	11.31	0.61	1495	0.32	MVB	BS in OCD
S1082	11.25	0.41	-	-	MVB	BS, poss. companion?
S1113	13.63	0.99	2.823	0.031	MVB	subsubgiant
S1237	10.78	0.94	697.8	0.105	MVB	eccentric binary
S1242	12.72	0.68	31.78	0.664	MVB	eccentric binary
S1234	12.65	0.57	4.36	0.06	MLG	triple

Table 1. Selected M67 stars identified with various observed samples. For S1234 the parameters are for the inner orbit.

puted by Kurucz (1992) from synthetic stellar spectra. This isochrone gives a good match between the MS hook and the observed gap in stars just below the end of the MS. It also gives a good fit to the giant branch (GB) and the red clump of stars on the zero-age horizontal branch, even with the uncertainties in the model atmospheres for cool stars used to compute the colour conversions. It should however be noted that an isochrone with $Z = 0.017$, $m - M = 9.75$ and $E(B-V) = 0.04$ gives an equally good match for the same age and other combinations can be found by varying the age.

3 BINARY POPULATION SYNTHESIS

To investigate the data in Figure 1 we consider a series of binary populations evolved from various initial distributions of orbital separations, mass-ratios and eccentricities in order to determine the number of blue stragglers produced. For each run we evolve two million binaries to an age of 10^{10} yr with the binary population synthesis code described by Hurley, Tout & Pols (2000). This code, which represents a thorough reworking of that presented by Tout et al. (1997), includes tidal circularization and synchronization, stellar rotation, angular momentum loss mechanisms, common-envelope evolution and supernova kicks, in addition to Roche-lobe overflow and mass transfer by a stellar wind.

Initially we vary only the separation distribution, taking the eccentricity as uniformly distributed. We choose the binary mass from the initial mass function (IMF) of Kroupa, Tout & Gilmore (1991, KTG1), by means of the generating function

$$\frac{M_{\rm b}}{\rm M_\odot} = 0.33 \left[\frac{1}{(1-X)^{0.75} + 0.04\,(1-X)^{0.25}} - \frac{(1-X)^2}{1.04} \right] , \quad (1)$$

where X is uniformly distributed between appropriate limits to give $0.2 \leq M_{\rm b}/\,{\rm M_\odot} \leq 100$. Because it has not been corrected for the effect of binaries it is more correctly used for total system mass. We then choose the component masses according to a uniform distribution of mass-ratio constrained by the single star limits of $0.1M_\odot$ and $50.0M_\odot$, i.e.

$$\max\left(0.1/\left(M_{\rm b}-0.1\right), 0.02\left(M_{\rm b}-50\right)\right) \leq q \leq 1\,. \quad (2)$$

We follow Eggleton, Fitchett & Tout (1989, hereinafter EFT) by taking the distribution of orbital separations expressed as

$$\left(\frac{a}{a_m}\right)^\beta = \sec\left(kW\right) + \tan\left(kW\right)\,, \quad (3)$$

where $W \in [-1, 1]$, and uniformly distributed and k satisfies

$$\sec k = \frac{1}{2}\left[\zeta^\beta + \zeta^{-\beta}\right]\,. \quad (4)$$

This distribution is symmetric in $\log a$ about a peak at a_m

Run	Z	Separation	e	q	$N_{\rm BS}$	$N_{\rm RS}$
PS1	0.02	EFT30	uniform	KTG1, uniform	1.1	1.9
PS2	0.02	EFT17	uniform	KTG1, uniform	1.9	2.4
PS3	0.02	EFT10	uniform	KTG1, uniform	3.2	2.7
PS4	0.02	FLAT LOG	uniform	KTG1, uniform	8.2	4.3
PS5	0.02	EFT10, max 200	uniform	KTG1, uniform	3.9	3.3
PS6	0.02	EFT10, max 200	thermal	KTG1, uniform	4.3	3.5
PS7	0.02	EFT10, max 200	uniform	KTG1, min 0.8	3.4	3.3
PS8	0.02	EFT10, max 200	uniform	KTG3	2.8	2.9
PS9	0.01	EFT10, max 200	thermal	KTG1, uniform	5.3	3.5

Table 2. Numbers are per 5 000 binaries, i.e. 10 000 stars, at 4.2 Gyr.

and ranges from a minimum separation of ζa_m to a maximum of a_m/ζ. We choose the constants ζ and β to be 10^{-3} and 0.33 respectively. A choice of $a_m \simeq 30$ AU corresponds to the Gaussian-like period distribution for nearby solar-like stars found by Duquennoy & Mayor (1991) which has a peak period $P \simeq 180$ yr.

The results are shown in Table 2 where EFTx represents separations chosen from eq. (3) with a peak, a_m, at xAU. The distribution flat in $\log a$ used in PS4 has the same limits as the EFT10 distribution of run PS3. For each run the number of BSs present at 4.2 Gyr per 5 000 binaries is shown. Our BSs are MS stars that have a mass at least 2% greater than the cluster turn-off mass at that time, defined as the stellar mass which is currently due to leave the MS. Also shown is the number of RS CVn stars, which may provide an additional constraint to the population. We define these as circular binaries with $P \leq 20$ d containing a sub-giant or giant primary losing mass in a wind, some of which is being accreted by the secondary. This ensures that the primary is rotating faster than it would as a single star at the same evolutionary stage so that the system is magnetically active.

We model another five populations using the EFT10 separation distribution with an upper limit of 200 AU. The peak at 10 AU in the distribution is still consistent with the Duquennoy & Mayor (1991) observations as is the maximum of 200 AU. This also agrees with the findings of Mathieu, Latham & Griffin (1990, hereinafter MLG) for 22 spectroscopic binaries in M67 while the maximum of 200 AU is greater than the hard/soft binary limit* (Heggie 1975) expected for an open cluster. Results for runs using EFT10 with varying choices for the eccentricity and mass-ratios are also given in Table 2. The IMF used in run PS8 is the single star IMF of Kroupa, Tout & Gilmore (1993, KTG3) and each binary component is chosen independently. The metallicity for each run is $Z = 0.02$ except for PS9 which examines the effect of using a lower value.

Run PS4 generates the most blue stragglers. We show in Section 5 that M67 probably contained about 40 000 stars initially: roughly 13 500 binaries with a 50% fraction. If all binaries that produce a BS are retained by the cluster then PS4 can explain the number found in M67. However, only about 25% of the BSs are in binaries, all of these have circular orbits, and practically none are found in binaries with periods greater than a year. So dynamical encounters during cluster evolution are required to explain BSs found in wide binaries and those found with eccentric orbits. Although the observations described by Abt (1983) are consistent with a flat distribution of $\log a$, more recent surveys (e.g. Duquennoy & Mayor 1991) favour a peaked distribution such as is used in all runs except PS4. The flat distribution has also been ruled out by EFT. Of the runs with a peaked distribution, PS6, with a thermal eccentricity distribution (Heggie 1975), produces the most BSs (excluding run PS9 which has lower metallicity). The initial systems in run PS6 that lead to the formation of BSs present at 4.2 Gyr are shown in Figure 3. Noticeably evident is the effectiveness of tidal circularization at bringing eccentric binaries close enough to make mass transfer possible. All instances of Case A mass transfer lead to coalescence of the two MS stars. Of the BSs produced by PS6 71.9% are single, 27.8% are in close binaries resulting from Case B mass transfer and only 0.3% are in wide binaries produced by Case C mass transfer or wind accretion. Figure 4 shows the mass distribution of BSs present at 4.2 Gyr. Binary evolution alone cannot explain BSs with mass greater than twice the cluster turn-off mass, such as F81 in M67.

The evolution of run PS6 is shown in Figure 1 for a 50% binary fraction and the assumption that binaries with mass-ratios less than 0.4 would be observed as MS stars. Even though the ratio of BSs to bright MS stars is decreas-

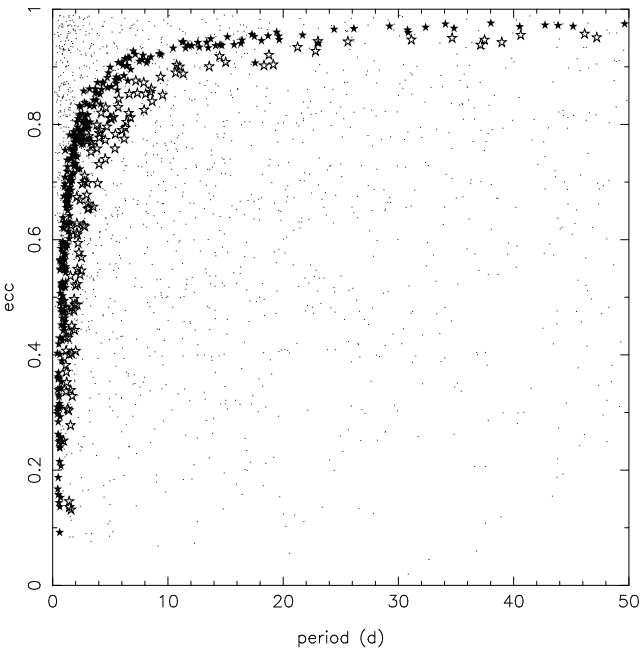

Figure 3. Eccentricity versus Period distribution showing the initial conditions that evolved to BSs via Case A mass transfer (solid stars, single stragglers) and via Case B mass transfer (open stars, stragglers in close circular binaries) for the run PS6. Note that some wide Case C mass transfer binaries were formed at $P > 50$ d.

* Heggie (1975) defined hard binaries to be sufficiently close that their binding energy exceeds the mean kinetic energy of the cluster stars. For binary component masses similar to the mean stellar mass of the cluster this roughly translates to a separation less than $a_{\rm hard} = 2r_{\rm h}/N$ where $r_{\rm h}$ is the half-mass radius and N is the number of cluster stars.

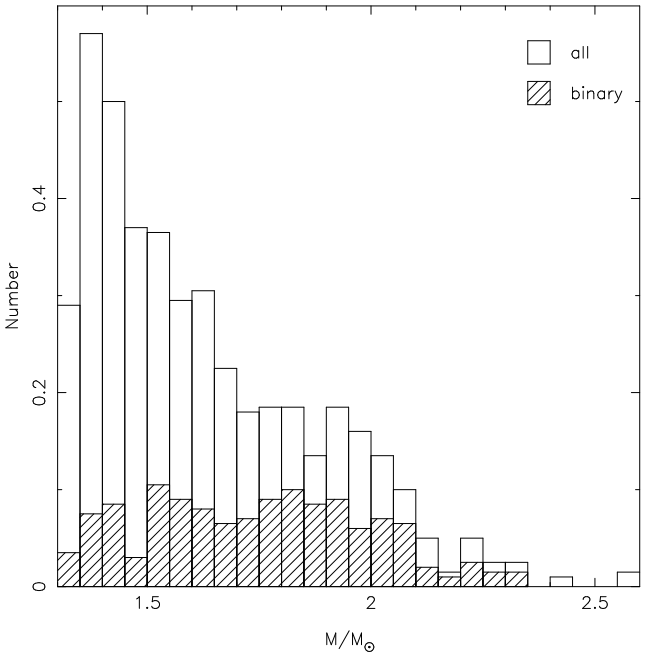

Figure 4. The distribution of stellar mass for blue stragglers at 4.2 Gyr in run PS6. The distribution is shown for all blue stragglers (hollow) and those that are in binaries (hatched). The cluster turn-off mass at this time is $M_{\rm TO} = 1.30\,{\rm M}_\odot$.

ing initially, the number of BSs produced actually increases with time. This is because increasingly more stars are evolving off the MS, growing in radius and interacting with their companion. Also, as time goes on, the masses of the progenitor stars that interact to produce BSs decreases so that the BS lifetime increases. After some time the number of BSs produced peaks. It then starts to fall, mainly as a result of a decreasing number of progenitor systems. The time of this peak is largely dependent on the ratio of the mean binary separation to the size of a star at the MS turn-off. The latter decreases with time and if stars do not grow to such large radii then binary interaction is less likely. Additionally, as this ratio increases, stars become more likely to fill their Roche-lobes on the GB, if at all, resulting in more cases of common-envelope evolution rather than steady mass transfer. We find the peak in $N_{\rm BS}$ for run PS6 occurs at about 5 Gyr quite unlike Pols & Marinus (1994) who found a peak at about 0.1 Gyr for a separation distribution flat in $\log a$. Their mass function was biased towards stars with $M > 2\,{\rm M}_\odot$ because they were interested in younger clusters. At 5 Gyr the turn-off mass drops below $1.25\,{\rm M}_\odot$ for the first time which means that the brighter MS stars begin to have radiative cores and therefore do not rejuvenate as much after mass transfer. As a result, BS lifetimes decrease in relation to MS lifetimes, contributing to the decrease seen in $N_{\rm BS}/N_{\rm MS}$ after 5 Gyr. Stars of lower metallicity have shorter MS lifetimes for $M \lesssim 9\,{\rm M}_\odot$ so that for a particular age the MS turn-off mass decreases with decreasing cluster metallicity. Run PS9 has a lower metallicity than PS6 and has a MS turn-off mass of $1.24\,{\rm M}_\odot$ at 4.2 Gyr. Consequently the peak in $N_{\rm BS}$ occurs at about this time which helps to explain why more BSs are produced at 4.2 Gyr than by PS6. Also, stars of the same mass grow to larger radii on the MS for lower metallicity so that binary interaction is more likely and $N_{\rm BS}$ in PS9 is always greater than in PS6.

Figure 1 shows that, as the population evolves, binary evolution alone cannot account for the number of observed BSs in open clusters if a realistic separation distribution is used. Cluster dynamics is therefore not only important for explaining BSs found in eccentric and/or wide binaries but is also required to increase the number produced. We can expect this theoretically through the hardening of primordial binaries, which increases the chance of mass transfer, as well as the possibility of collisions between MS stars in the cluster core. In addition, dynamical evolution together with the effects of a tidal field alters the cluster mass function as low-mass stars are stripped preferentially from the outer regions (Terlevich 1987).

A problem with all of the population synthesis runs is that the number of RS CVn systems is comparable to the number of BSs, whereas the observations suggest that there should only be one for every four BSs. This is most likely another signature of the cluster dynamics. Giant stars present a much larger cross-section for collisions than MS stars and are therefore more likely to be involved in dynamical encounters (even though their existence is shorter). Moreover, the hardening of close binaries and the disruption of wide binaries both act to reduce the number of RS CVn systems.

4 THE *N*-BODY CODE

The study of star clusters is currently at a very exciting stage. Observationally the improved resolution of the Hubble Space Telescope (HST) is providing a wealth of high-quality information on clusters and their stellar populations (e.g. Guhathakurta et al. 1998; Piotto et al. 1999). This includes the dynamically old globular clusters which populate our Galaxy as well as those of the Magellanic Clouds which exhibit a wide range of ages. Coupled to this are the recent advances in computer hardware which have brought the possibility of direct globular cluster modelling within reach for the first time (Makino 1999).

In practice the direct integration of an N-body system presents many technical challenges and has only limited applicability to real clusters because the required value of N is too large for a simulation to be completed in a reasonable time. As a result, most N-body simulations performed so far have involved a varying number of simplified and unrealistic conditions, such as including only single stars, using only equal-mass stars, neglecting stellar evolution or assuming no external tidal field (e.g. McMillan, Hut & Makino 1991; Heggie & Aarseth 1992). Despite the fact that, even with simplified conditions, direct N-body simulations are limited to N considerably less than is needed for globular clusters, much can still be learnt by scaling the results with particle number, or by modelling small open clusters. The scaling of time depends essentially on the mechanism to be modelled (Meylan & Heggie 1997) but unfortunately the various timescales scale differently with N so complications arise when competing processes are involved. Aarseth & Heggie (1998) discuss these problems further and present a hybrid time-scaling method which can cope with the transition from early evolution related to the crossing time to later relaxation-dominated evolution.

A complication in the use of the results of small-N calculations to make inferences relating to larger clusters is that many of the structural properties are N-dependent (Goodman 1987). Also energy considerations which may be dominant for small-N, such as the binding energy of a single hard binary, may not be significant for a larger system where only the overall energetics is important. Another problem is that, as N decreases, the results become increasingly noisy owing to statistical fluctuations. Casertano & Hut (1985) have studied how noise affects determination of the core parameters while Giersz & Heggie (1994) have suggested that the situation may be alleviated by averaging the results of many simulations. The validity of the results of N-body calculations has been challenged on a fundamental level by Miller (1964) who showed that two N-body systems integrated from similar initial conditions diverge exponentially. Quinlan & Tremaine (1992) note that this instability occurs on a timescale comparable with the crossing time, making the results of N-body integrations extremely sensitive to numerical errors and therefore unreliable over relaxation timescales. However, they also find that the numerical orbits of N-body models are *shadowed* by real systems even though their initial conditions differ.

Ultimately the N-body approach remains the method of choice for creating dynamical models of star clusters because a minimum number of simplifying assumptions are required and it is relatively easy to implement additional realistic features. For a comprehensive description of the various methods for dynamical star cluster modelling see Meylan & Heggie (1997), or Hut et al. (1992).

The N-body code we use is `NBODY4`, versions of which have been described in the past by Aarseth (1996, 1999a, 1999b). This code has been adapted to run on the HARP-3 special-purpose computer (Makino, Kokubo & Taiji 1993) and makes use of the many advances made in the field since publication of the original direct N-body code (Aarseth 1963).

4.1 Integration

In N-body simulations it is usual to choose scaled units (Heggie & Mathieu 1986) such that $G = 1$, the mean mass is $1/N$ and the virial radius is unity. This means that, in N-body units, the initial energy of the system in virial equilibrium is $-1/4$ and the crossing time is $2\sqrt{2}$. The N-body units can be scaled to physical units via the total stellar mass and an appropriately chosen length-scale factor. In this work we do not model the initial phase of cluster evolution, the formation of the cluster. Instead the initial conditions are chosen subject to suitable observational constraints and we then integrate a system in virial equilibrium forward in time. Basic integration of the equations of motion is performed by the Hermite scheme (Makino 1991) developed specifically for the HARP. This scheme employs a fourth-order force polynomial and exploits the fast evaluation of the force and its first time derivative by the HARP. It is more accurate than the traditional divided difference formulation (Ahmad & Cohen 1973; Aarseth 1985) of the same order and has advantages in simplicity and performance.

To exploit the fact that stellar systems involve a wide range of particle densities, and thus that different particles will have different timescales for significant changes to their orbital parameters, it is desirable to introduce individual time-steps. The individual time-step scheme requires the coordinate and velocity predictions to be performed for all other particles at each force evaluation. Fortunately the overheads that this introduces are reduced by utilizing the HARP hardware for fast predictions to first order. Significant gains in efficiency are also achieved by adopting quantized hierarchical time-steps. Although first developed by McMillan (1986) to optimize vectorization of N-body codes, the method also aids efficient parallelization of the force calculations. The advantage of quantized time-steps is that a block of particles can be advanced at the same time so that only one prediction call to the HARP is required for each block.

4.2 Close Encounters and Regularization

When a binary system is within an environment such as a star cluster where gravitational encounters with other bodies are possible it is not sufficient to describe the orbit by averaged quantities, as used for isolated systems in binary population synthesis (Hurley, Pols & Tout 2000). Instead the orbit must be integrated directly, in a way that enables the positions of both stars to be known at any time. This is complicated by the fact that the orbital characteristics are affected by perturbations from the attractive forces of nearby stars. If the relative separation of the two binary stars is $\mathbf{R}$ then

$$\ddot{\mathbf{R}} = -\frac{M_{\rm b}}{R^3}\mathbf{R} + \mathbf{P} \qquad (5)$$

describes the motion where $\mathbf{P}$ represents the external tidal perturbations. As $\mathbf{R} \rightarrow 0$ this equation becomes strongly singular, leading to increasing errors and small time-steps if integrated by standard methods. Therefore alternative methods which regularize the equations of motion for close encounters, or make use of a hierarchical data structure, must be employed. This includes the case of two strongly interacting particles in a hyperbolic encounter. `NBODY4` makes use of KS regularization (Kustaanheimo & Stiefel 1965) which treats perturbed two-body motion in an accurate and efficient way. A recent development has seen the introduction of the Stumpff KS scheme (Mikkola & Aarseth 1998) which achieves a high accuracy without extra cost. This scheme, also incorporating the so-called slow-down principle based on adiabatic invariance, is now used in `NBODY4` and requires about 30 steps per orbit to obtain high accuracy when relatively weak perturbations are involved.

Since all the KS integrations are carried out on the host machine rather than the HARP, and each orbit may require many KS steps, the treatment of many perturbed systems is often the most expensive part of the simulation. Therefore the extent of the primordial binary population, and its distribution of periods, is a major consideration when determining the size of a simulation that can be completed in a reasonable time. For perturbed two-body motion, only contributions from relatively nearby particles need be considered because the tidal force varies as $1/r^3$. If no perturbers are selected for a KS pair at apastron then unperturbed KS motion is assumed and the system can be advanced one or more periods without stepwise integration. Because hard (i.e. close) binaries are less likely to be perturbed, a signif-

icant number of such binaries among the primordial population can reduce the load on the host machine. Thus the choice of period distribution is once again a prime consideration.

To cope with strong interactions between close binaries and single stars the KS treatment has been extended to three-body regularization (Aarseth & Zare 1974). This basically requires two KS regularizations coupled by suitable coordinate transformations. A further generalization to include a fourth body led to the formulation of chain regularization (Mikkola & Aarseth 1990, 1993). The essential feature of this challenging treatment is that dominant interactions along the chain of particles are modelled as perturbed KS solutions and all other attractions are included as perturbations. This is ideal for treating compact subsystems and is currently used in `NBODY4` for configurations of three to six bodies.

4.3 Stellar Evolution Treatment

To provide realistic cluster models the simulation must be able to account for changes to the radii and masses of stars during the lifetime of a star cluster. The evolution of the single and binary stars must be performed in step with integration of the dynamics so that interaction between the two processes is modelled consistently. The earlier version of `NBODY4` included stellar evolution in the form of the algorithms presented by Tout et al. (1997) but this treatment is only relevant to stars of Population I composition. It is also based on stellar models which have since been superseded by the models of Pols et al. (1998) incorporating, among others, improvements to the equation of state, updated opacity tables, and convective overshooting. We have now incorporated the updated stellar evolution treatment described by Hurley, Pols & Tout (2000), valid for all metallicities in the range $Z = 10^{-4}$ to 0.03, into `NBODY4` in its entirety. This means that the metallicity of our cluster models can be varied and that a more detailed and accurate treatment of all the single star evolution phases is used. Variations in composition can affect the stellar evolution timescales as well as the appearance of the evolution in a CMD and the ultimate fate of a star.

All stars carry with them a set of variables that describe their evolutionary state. These are the initial mass (M_0), current mass (M_t), stellar radius (R_*) and stellar type (k_*). Other physical parameters, such as the luminosity and core mass, are not saved for each star because these are required less frequently and are calculated when needed.

Because the stars evolve at different rates, depending on their evolutionary stage and mass, they require different frequencies for the updating of their variables. Each star has the associated variables $T_{\rm ev}$ and $T_{\rm ev0}$ which represent the next stellar evolution update time, and the time of the last update, respectively. Whenever $T \geq T_{\rm ev}$, where T is the simulation time, the star is updated by the stellar evolution algorithms. The value of $T_{\rm ev}$ is then advanced by a suitable choice of time-step Δt which depends on the evolutionary stage of the star (see Hurley, Pols & Tout 2000) and ensures that the physical parameters change sufficiently smoothly. After Δt is chosen we check whether the stellar radius will change by more than 10% over the interval and reduce Δt if this is the case. In practice the stellar evolution algorithms are not called continuously because successive calls to the main routine which controls the treatment are limited by a minimum time interval, which is fairly small. This means that one call to the routine can involve the updating of many stars and that an individual star may be advanced several times within one call if it is in a particularly rapid stage of evolution.

In the simulation all stars have evolved for the same amount of time, i.e. the age of the cluster, but they may have different relative ages, for example if a star has been rejuvenated by mass transfer. Also, when a remnant stage is begun, such as a helium star, white dwarf (WD), neutron star (NS) or black hole (BH), the age of the star is reset to zero for the new type. Therefore the additional variable EPOCH is introduced for each star so that its age at any time is given by the difference between the current cluster age and its EPOCH.

We include mass loss by stellar winds according to the prescription given in Hurley, Pols & Tout (2000). The timestep is limited so that a maximum of 2% of the stellar mass can be lost. Any mass lost which is not accreted by a close companion is assumed to leave the cluster instantaneously, with the appropriate corrections made to account for the change in potential energy, maintaining energy conservation for the system. The force on nearby stars must also be modified as a result of the mass change or, if a significant amount of mass is lost, a complete re-initialization of the force polynomials on the HARP may be required. Also, if a NS or BH is formed, a velocity kick taken from a Maxwellian distribution with dispersion $\sigma = 190\,{\rm km\,s^{-1}}$ (see Hurley, Tout & Pols 2000) is given to the supernova remnant which is usually enough to eject it from the cluster.

4.4 Binary Evolution Treatment

For the treatment of evolution within a binary system we include the features described in Hurley, Tout & Pols (2000) over and above those of the old algorithms (Tout et al. 1997). However, we use the treatment of tidal circularization developed by Mardling & Aarseth (2000, hereinafter MA) which includes features that cope with the added complication of external perturbations to the orbital parameters, and has been implemented to work closely with the KS scheme.

Each binary has an associated composite particle, the centre-of-mass (CM) particle, which has its own set of variables, M_t, k_*, $T_{\rm ev}$ etc., as well as additional variables such as the binding energy per unit mass of the system. A typical binary will make a journey through a series of CM evolution stages, beginning with $k_{*,\rm CM} = 0$ when it is first created: either primordially or during the evolution. A close binary orbit circularizes tidally as energy is dissipated but angular momentum is conserved. Tidal circularization ($k_{*,\rm CM} = -2$) is activated when the circularization timescale of the binary is less than 2×10^9 yr. Note that the intrinsic stellar spin is not incorporated in the circularization treatment so that the angular momentum of an unperturbed binary orbit remains constant during the circularization process. This could be rectified in line with the tidal model of Hurley, Tout & Pols (2000).

For a binary of high eccentricity it is possible for the energy exchange between the orbit and the tides at periastron to become chaotic ($k_{*,\rm CM} = -1$). This means that oscilla-

tions occur which gradually damp the system until sufficient energy is dissipated for the *chaos boundary* to be crossed, when the orbit settles on some eccentricity whence angular momentum is conserved, and the orbit begins to circularize (MA). The implementation is based on a non-linear dissipation timescale and assumes conservation of total angular momentum for the system (i.e. the stars spin up). Chaotic behaviour is most likely to occur in tidal-capture binaries and MA note that it is still not clear how stars in chaotic orbits respond to the huge tidal energies involved. Tout & Kembhavi (1993) and Podsiadlowski (1996) have shown that the response of the tidally heated primary depends on the region of the star in which the energy is deposited and also the timescale on which this energy is thermalized within the star.

Once the circularization is complete ($k_{*,\rm CM} = 10$) the binary is tested regularly for Roche-lobe overflow (RLOF). Prior to circularization the unlikely possibility of RLOF is ignored. In most cases this technicality does not lead to any physical irregularities because tidal interaction generally acts to remove any eccentricity on a timescale shorter than the evolution timescale of the binary. However problems may arise if a system forms in a close eccentric orbit. Even then there is evidence that some circularization occurs during the formation process (Mathieu 1994). While the orbit is circularizing the stars are also evolving and growing in radius, so contact is expected in some systems as the orbit approaches zero eccentricity. However the timescale for a collision is actually prolonged because the periastron distance grows as e shrinks, owing to conservation of angular momentum. Thus, as the stars are expanding so is the minimum separation between them. Also most binaries do not begin to circularize, or to come close to a RLOF state, until one of the stars is on the GB or AGB, at which point it is losing mass in a stellar wind that causes an additional increase in the separation. Nevertheless, stages of rapid radius growth may result in premature coalescence.

It is also possible for the eccentricity of a binary to increase as a result of external perturbations acting on the orbit. If this induces an eccentricity in an orbit which was previously circular the binary is reset to standard type ($k_{*,\rm CM} = 0$). This is also done if an eccentric binary survives one of the component stars exploding as a supernova to leave a NS or BH remnant.

While a binary is in a detached state the stars are updated in the same way as single stars. The only difference is that both stars must be treated at the same time so that the possibility of wind accretion can be modelled. If the CM type is $k_{*,\rm CM} = 10$ or greater, each time the binary stars are updated the time until the primary star fills its Roche-lobe is estimated. This is used to set $T_{\rm ev,CM}$. If at any stage $T \geq T_{\rm ev,CM}$ then RLOF could have begun and the binary is subject to the ROCHE procedure ($k_{*,\rm CM} = 11$) where it is evolved forward according to the treatment described in Hurley, Tout & Pols (2000). This means that the physical time of the binary evolution can move slightly ahead of the cluster integration time, introducing the need for coasting periods in which the binary is put on hold until the dynamical integration time catches up. The amount of time that the binary moves ahead during ROCHE is determined by physical conditions of the components. Any stellar wind mass loss during RLOF is also dealt with inside ROCHE so it is important that $T_{\rm ev}$ for each of the component stars is greater than the time reached by the binary when it exits the active RLOF stage, i.e. $T_{\rm ev,CM} < T_{\rm ev,1}, T_{\rm ev,2}$. In this way the component stars have their evolution treated as part of the RLOF process and not as individuals. A sustained phase of RLOF may involve a series of active ROCHE calls each followed by a coasting period. It is also possible that a binary may experience more than one phase of RLOF during its evolution. This is easily accommodated by the treatment. During mass transfer the separation of the binary stars changes and the KS variables are updated frequently. As a fundamental variable for two-body regularization the binding energy per unit mass must be determined accurately at all times. In fact, all the KS variables must be corrected for mass loss. A mass-loss correction is also made to the total energy of the cluster and the force polynomials of nearby stars are re-initialized.

We treat common-envelope evolution and collisions that arise as a result of contact systems as part of the ROCHE process. In general, direct stellar collisions during the cluster evolution are very rare because the interacting stars most likely form a tidal capture binary, which may be quickly followed by coalescence via a common-envelope or contact phase. This is due to the relatively low velocity dispersion, $\sigma \simeq 10\,{\rm km\,s^{-1}}$, of cluster stars. In galactic nuclei where typically $\sigma \simeq 100\,{\rm km\,s^{-1}}$ direct collisions are expected. We use a periastron criterion, derived for main-sequence stars (Kochanek 1992),

$$a\,(1-e) \;<\; 1.7\left(\frac{M_1+M_2}{2M_1}\right)^{1/3} R_1\,, \qquad (6)$$

where R_1 is the primary radius, to determine direct collisions.

Because common-envelope events and collisions frequently lead to coalescence, either one or two particles can become redundant. Similarly some single star supernovae may not leave a remnant. In such cases it is simplest to create a massless component and place it well outside the cluster so that it escapes soon. If the component of a binary is removed then the coalescence product is given the CM coordinates and velocity of the original binary. Energy corrections associated with mass loss are performed and a new force polynomial initialized.

As already mentioned, the fraction of the stars in primordial binaries is of great importance. It is generally accepted that some degree of primordial population is present because the rate of binary formation during the evolution would not be enough to halt core-collapse appreciably (Hut et al. 1992). Binary stars in clusters can also be identified through their position in the CMD of the cluster as the combination of light from the two stars displaces the binary from the position of a single star having the same mass as either of the components (Hurley & Tout 1998). This is most noticeable on the MS where the existence of a distinct binary sequence has been exploited by the resolution of the Hubble Space Telescope (HST) to reveal globular cluster binary fractions of 10 to 30% (e.g. Richer et al. 1997; Elson et al. 1998). For open clusters results are often uncertain because the number of stars is smaller and membership can be difficult to determine. Even so, a significant number of pre-main-sequence binaries and multiple systems have been

found in young open clusters and associations (e.g. Simon et al. 1995; Brandner et al. 1996).

4.5 Hierarchical Systems

During the evolution of a star cluster stable multiple systems can form as a result of dynamical interactions. The formation of hierarchical triples, in which one component of a binary is itself a binary, has been shown to occur in various scattering experiments (e.g. Mikkola 1983; Bacon, Sigurdsson & Davies 1996) mainly as a result of strong binary-binary encounters. The inner binary of such a system may be relatively hard so that integration of the strongly perturbed KS solution can prove to be extremely time-consuming. This is especially true if the hierarchy is stable for a long period of time. In that case the inner binary only experiences short-term fluctuations in its orbital parameters, and so it is acceptable to perform direct integration only of the outer orbit while the system remains stable.

A semi-analytical stability criterion based on the analogy with the chaos boundary in tidal evolution has been presented by MA and implemented in `NBODY4`. They employ a critical periastron distance for the outer orbit in terms of the inner semi-major axis, $a_{\rm in}$, given by

$$R_{\rm p,crit}^{\rm out} = C \left[(1+q_{\rm out}) \, \frac{(1+e_{\rm out})}{(1-e_{\rm out})^{1/2}} \right]^{2/5} a_{\rm in} \, , \qquad (7)$$

where $e_{\rm out}$ is the eccentricity of the outer orbit and $C \simeq 2.8$ is determined empirically. The mass-ratio of the outer orbit is $q_{\rm out} = M_3/(M_1+M_2)$, where M_1 and M_2 are the component masses of the inner orbit. If the outer periastron separation is greater than $R_{\rm p,crit}^{\rm out}$ we consider the hierarchy to be stable and temporarily merge the stars into one KS system consisting of the CM particle of the inner binary and the third body, M_3. Because the period of the outer orbit is considerably longer than that of the inner orbit this procedure greatly reduces the computational cost. Quadruple and higher-order systems are similarly dealt with. Procedures to model the cyclic oscillations of the inner eccentricity, the Kozai effect (Kozai 1962), and any tidal circularization that is induced, are implemented according to MA.

The possibility of an exchange interaction, in which one of the inner binary components is displaced by an incoming third star, is checked by the criterion of Zare (1977)†. As noted by Aarseth (1999a), the stability boundary lies above the exchange boundary when all the masses involved are comparable and the two only begin to overlap when $q_{\rm out} \simeq 5$. If an exchange does occur then the expelled star invariably leaves the three-body system altogether.

To ease the book-keeping required when particles are regularized or hierarchies are formed, the simulation particles are kept in an ordered data list throughout the evolution. Consider a model composed of $N_{\rm s}$ single stars and $N_{\rm b}$ regularized binaries, i.e. $N = N_{\rm s} + 2N_{\rm b}$ stars in total. The first $2N_{\rm b}$ entries in the data list are the binary stars, with each binary pair grouped together, followed by the $N_{\rm s}$ single star entries, and finally the $N_{\rm b}$ CM particles. Take the case of a basic KS binary which is combined with a single star to form a stable hierarchy. The single star is moved to the position formerly occupied by the second component of the binary and the CM particle of the old binary is moved to the first component position. The values, such as binding energy, of the old binary CM are moved to the position formerly occupied by the single star which now has zero mass and is a *ghost* particle, i.e. it does not contribute to force calculations. Component masses of the inner binary are saved in a merger table and the CM position for the binary now holds variables relevant to the outer orbit. If the hierarchy is broken up then all the variables are easily re-assigned and the inner binary restored. Possible reasons for termination of a hierarchy include violation of the stability criterion or the onset of RLOF in the inner binary. If the hierarchy involves the merger of two binaries then both CM particles would be the components of the new binary.

† Because of the degeneracy of angular momentum, this criterion is only used for small inclinations

5 ESCAPE FROM A TIDALLY-LIMITED CLUSTER

Fan et al. (1996) present CCD spectrophotometry of 6 558 stars in the field of M67. They estimate that the MS is complete down to $0.5M_\odot$ and that the cluster has a total observed mass of approximately $1\,000M_\odot$ in stars with masses greater than $0.5M_\odot$. The observations reveal a mean (projected) half-mass radius of 2.5 pc for MS stars compared with 1.6 pc for the (more centrally condensed) BS population. The tidal radius is at 10 pc and their data is consistent with a 50% binary fraction.

With an initial population comprising single star masses chosen from the KTG3 IMF, binary masses from the KTG1 IMF and a 50% binary fraction, about 7 000 stars ($3\,500M_\odot$) are required to give a current cluster mass of $2\,500M_\odot$ (corresponding to $1\,000M_\odot$ observed above $0.5M_\odot$). The mass loss is due solely to stellar evolution and assumes no dynamical effects on the population. However, in a cluster environment stars undergo gravitational interactions so that from time to time an encounter gives enough energy to a star that it can escape from the system. The timescale over which the stars evaporate in this way is related to the relaxation timescale, $t_{\rm r}$, of the cluster and is shortened by the presence of an external tidal field as well as the inclusion of a full spectrum of stellar masses.

An isolated spherical cluster with potential Φ has an escape speed $v_{\rm e}$ at radius r given by

$$v_{\rm e}^2 = -2\Phi\,(r) \, . \qquad (8)$$

The mean-square escape speed in a system with uniform density is

$$\langle v_{\rm e}^2 \rangle = 4 \langle v^2 \rangle \, , \qquad (9)$$

so the RMS escape speed is twice the particle RMS speed. For a Maxwellian velocity distribution the fraction of particles that have speeds exceeding twice the RMS speed is $\gamma = 7.4 \times 10^{-3}$ (see Binney & Tremaine 1987, p. 490) and the evaporation process can be approximated by removing a fraction γ of stars each relaxation time, i.e.

$$\frac{dN}{dt} = -\gamma \, \frac{N}{t_{\rm r}} \, . \qquad (10)$$

Evaporation then sets an upper limit to the lifetime of the bound stellar system of about $10^2 t_{\rm r}$. Note that numerical solution of the Fokker-Planck equation gives $\gamma = 8.5 \times 10^{-3}$ (Spitzer 1987, p. 54). The total energy of a cluster with total mass M and radius R is, according to the virial theorem,

$$E = -k\frac{GM^2}{R}\,, \tag{11}$$

where k is a dimensionless constant of order unity. If it is assumed that the cluster evolution is self-similar, so that its shape remains fixed, k is independent of time. Since evaporation is mostly driven by weak encounters the stars escape with very little energy so that E remains essentially fixed. Therefore

$$\frac{r}{r_0} = \left(\frac{M}{M_0}\right)^2 \tag{12}$$

and the cluster contracts as it loses mass.

The evolution of a real star cluster is somewhat different to that of an isolated uniform system because the cluster is subject to the tidal force of the galaxy in which it resides. Consider a cluster in a circular orbit around a galaxy at a distance $R_{\rm G}$ from the galactic centre. To estimate the strength of the tidal field exerted on the cluster we assume that $M_{\rm G}$, the galactic mass enclosed by the orbit, is distributed throughout the inner spherical volume. By choosing the origin of a rotating reference frame to be the cluster centre-of-mass, the x-axis directed away from the galactic centre, the y-axis in the direction of rotation, and linearizing the tidal field, the equations of motion are

$$\ddot{x} = F_x + 2\omega_{\rm G}\dot{y} + 3\omega_{\rm G}^2 x$$
$$\ddot{y} = F_y - 2\omega_{\rm G}\dot{x} \tag{13}$$
$$\ddot{z} = F_z - \omega_{\rm G}^2 z \tag{14}$$

(Giersz & Heggie 1997), where

$$\omega_{\rm G} = \sqrt{\frac{GM_{\rm G}}{R_{\rm G}^3}} \tag{15}$$

is the angular velocity. The tidal radius $r_{\rm t}$ of the cluster is defined by the saddle point on the x-axis of the effective cluster potential, analogous to the definition of the Roche-lobe radius in a binary system (except that the cluster is not co-rotating with its orbit).

The Galactic tidal field can conveniently be described in terms of Oort's constants,

$$A = 14.5 \pm 1.5\,{\rm km\,s^{-1}\,kpc^{-1}}$$
$$B = -12 \pm 3\,{\rm km\,s^{-1}\,kpc^{-1}}$$

(Binney & Tremaine 1987, p. 14), so that

$$A - B = \left(\frac{v_{\rm G}}{R_{\rm G}}\right)_{R_0} = 26.5 \pm 4\,{\rm km\,s^{-1}\,kpc^{-1}}\,. \tag{16}$$

This is consistent with an orbital velocity of $v_{\rm G} = 220{\rm km\,s^{-1}}$ (Chernoff & Weinberg 1990) at $R_0 = 8.5\,{\rm kpc}$. In this formulation the tidal radius is

$$r_{\rm t} = \left(\frac{GM}{4A\,(A-B)}\right)^{1/3}\,. \tag{17}$$

The cluster escape rate can be expressed by

$$\frac{dM}{dt} = -\frac{k_{\rm e}}{\log_{10}\Lambda}\frac{M}{t_{\rm rh}} \tag{18}$$

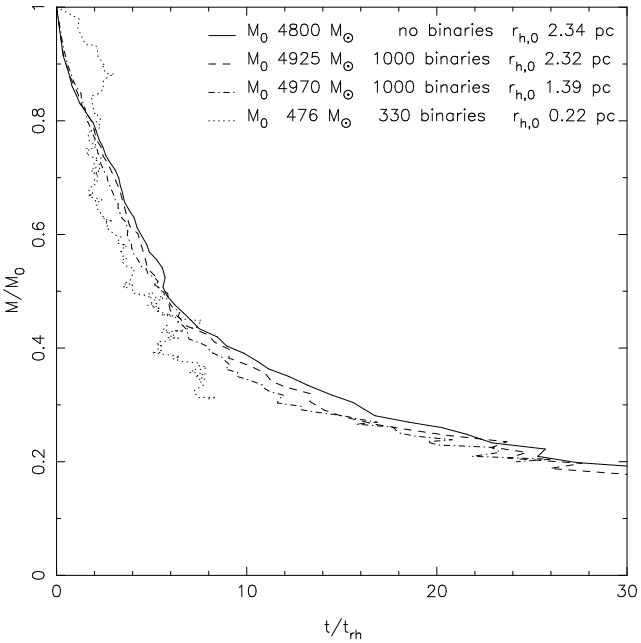

Figure 5. Evolution of the total mass of bound stars for N-body models started with 10 000 stars and a standard tidal field with the time scaled by the current half-mass relaxation time of the cluster. Also shown is the evolution for a model started with only 1 000 stars but with a 50% binary fraction.

where M is the cluster mass at time t for N stars, $\Lambda = 0.4N$ is used in the Coulomb logarithm and

$$t_{\rm rh} = 0.894\,\frac{N}{\log_{10}\Lambda}\,\frac{r_{\rm h}^{3/2}}{M^{1/2}}\ {\rm Myr} \tag{19}$$

is the half-mass relaxation time if $r_{\rm h}$ is in pc and M in $M_\odot$. The constant $k_{\rm e}$ quantifies the rate of mass lost in stars stripped from the cluster, where $\gamma = k_{\rm e}/\log_{10}\Lambda$ because $M \propto N$. Numerical solution of the Fokker-Planck equation for a tidally truncated cluster gives $\gamma = 4.5 \times 10^{-2}$ (Spitzer 1987, p. 59).

We have investigated cluster escape rates for simulations with a full mass spectrum, mass loss from stellar evolution and a standard Galactic tidal field ($v_{\rm G} = 220\,{\rm km\,s^{-1}}$ and $R_{\rm G} = 8.5\,{\rm kpc}$), in a series of N-body models evolved with `NBODY4`. In these simulations we assume the stars are stripped from the cluster when $r > 2r_{\rm t}$. This underestimates slightly the escape rate compared to letting them escape when they are outside the tidal radius (Giersz & Heggie 1997). We performed a total of six simulations starting with $N = 10\,000$. In each model the initial positions and velocities of the stars are assigned according to a Plummer model (Aarseth, Hénon & Wielen 1974) in virial equilibrium with the tidal radius defined by eq. (17). The single star masses are chosen from the KTG3 IMF and the binary masses from the KTG1 IMF, with minimum and maximum single star limits of 0.1 and $50\,{\rm M}_\odot$. We set the distribution of mass-ratios for the binaries to be uniform between 0.1 and 1 and the metallicity at $Z = 0.02$. We choose the binary separations from the same distribution as population synthesis run PS1. Three of the simulations had no primordial binaries and a length scale chosen so that $r_{\rm h,0} \simeq 0.1 r_{\rm t,0}$. The

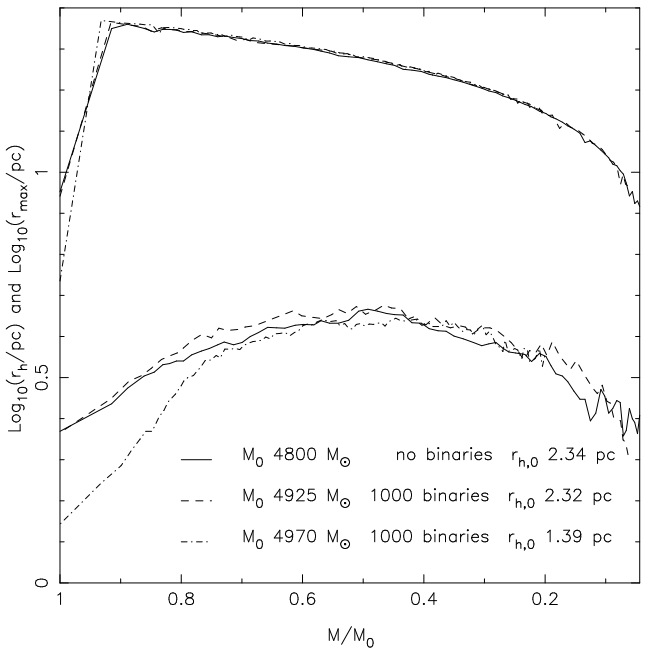

Figure 6. Evolution of the maximum and half-mass radii for the same $N = 10\,000$ models as in Figure 5. Note that the maximum radius is given by the radius of the star closest to the tidal radius. It quickly approaches the tidal radius following the initial expansion of the cluster. Since stars are not removed from the cluster until $r > 2r_{\rm t}$ there is a small population of cluster members with $r_{\rm max} < r < 2r_{\rm t}$. On average the mass in cluster stars outside the tidal radius is less than 2% of the total cluster mass.

other three had a primordial binary fraction of $f_{\rm b} = 0.11$[‡]: two of these with the same initial half-mass radius as the single star models and one, started with $r_{\rm h,0} \simeq 0.06 r_{\rm t}$, more condensed. In each simulation the initial cluster mass, M_0, is about $5\,000\,{\rm M}_\odot$ which gives a tidal radius of about 22 pc.

The evolution of the cluster mass as a function of the number of half-mass relaxation times is shown in Figure 5. The inclusion of binaries has little effect, nor does varying the initial concentration of the cluster, as long as the time is scaled by the current half-mass relaxation time. In fact the initial size has little effect because, owing to mass loss from massive stars and core contraction, the cluster quickly expands to fill its tidal radius which depends only on mass. This is demonstrated in Figure 6 which shows the variation of the half-mass radius with cluster mass as well as the position of the star closest to the tidal radius at the time. As each cluster evolves, the half-mass radius, which initially expands freely, starts to feel the effect of the contracting tidal radius so that the rate of expansion slows. Eventually the half-mass radius begins to contract and the cluster evolution becomes remarkably self-similar. For each simulation the turn-over occurs at $M/M_0 \simeq 0.5$ when $t/t_{\rm rh} \simeq 6$. During the subsequent self-similar evolution phase the ratio of the tidal and half-mass radii is $r_{\rm t}/r_{\rm h} \simeq 4$.

The mean core-collapse (CC) time for all the models is $t_{\rm CC} \simeq 4t_{\rm rh}$. In terms of the initial half-mass relaxation time this is $t_{\rm CC} \simeq 7t_{\rm rh,0}$ because $t_{\rm rh,CC} \simeq 2.2t_{\rm rh,0}$ owing to the initial expansion of $r_{\rm h}$. At the time of core-collapse an average of five hard binaries have formed in the core of the single star models. The model with the smaller $r_{\rm h,0}$ reached the $r_{\rm h}$ turn-over point in about 85% of the time it took the lower density models but this single result is not significant.

From the $N = 10\,000$ models we find that $k_{\rm e} \simeq 0.3$ fits the data adequately for almost the entire cluster evolution. This result is consistent with a series of six $N = 1\,000$ simulations that we began with $f_{\rm b} = 0.5$ and $r_{\rm h,0} \simeq 0.03 r_{\rm t}$. For these smaller models the half-mass radius starts to contract at $M/M_0 \simeq 0.5$. The mass-loss rate is also compatible with the results of Giersz & Heggie (1997) from a series of N-body models with $N = 500$, when we take into account the fact that Plummer models have a lower escape rate than King models. This is due to Plummer models having a slightly weaker tidal field, and therefore evolving more slowly in the post-core-collapse phase of evolution, than their King model counterparts. Giersz & Heggie (1997) use a minimum mass of $0.4\,{\rm M}_\odot$, compared to the value of $0.1\,{\rm M}_\odot$ in the models presented here, so they have a higher proportion of massive stars. Their shorter evolution timescales cause the simulations to evolve faster which increases the escape rate and partly explains why their value of $k_{\rm e} \simeq 0.6$ (converted to the units used here assuming $\Lambda = 0.4N$ for both sets of models) is larger. Giersz & Heggie (1997) found that $\Lambda = 0.015N$ is required to make the results of their models agree with the Fokker-Planck models of Chernoff & Weinberg (1990), in which case the conversion of their escape rate gives an even larger value of $k_{\rm e} \simeq 1.5$.

So how robust is our $k_{\rm e}$ against changes to the initial conditions assumed for the N-body models? We have already discussed that it is sensitive to the model from which the density and velocity profiles are taken: Plummer, King or otherwise. The mass function used also has an effect even though a change in IMF slope will be offset to some degree by the inverse dependence of the relaxation timescale on average stellar mass. Our escape rate has been derived by considering a number of model sizes and binary fractions but must be tested over a greater range of parameter space before it can be universally accepted. Factors such as the proportion of hard binaries must also have an, as yet undetermined, effect on the result. Caution should be exercised when applying $k_{\rm e}$ to situations where the initial conditions differ substantially with those from which it was derived.

If the evolution of the cluster is self-similar then

$$\left(\frac{r_{\rm h}}{r_{\rm h,0}}\right) = \left(\frac{M}{M_0}\right)^{2-\zeta}, \qquad (20)$$

which stems from writing the rate of change of the total cluster energy as

$$\frac{dE}{dt} = \frac{\zeta E}{M}\frac{dM}{dt}. \qquad (21)$$

If $\zeta > 2$, $r_{\rm h}$ increases as M decreases. This can occur during the initial violent relaxation phase when stellar wind mass-loss causes an overall expansion, or during the post-core-collapse expansion of the inner regions. If $\zeta = 5/3$ then the evolution of the half-mass radius follows the decrease in tidal radius as the cluster evolves. Using eq. (20) to integrate eq. (18) gives

‡ We define the binary fraction as $f_{\rm b} = N_{\rm b}/(N_{\rm b} + N_{\rm s})$ for $N_{\rm b}$ binaries and $N_{\rm s}$ single stars. During this work we may also refer to a binary fraction as a percentage, i.e. $f_{\rm b} = 50\%$, and we note that this should more correctly be called a binary frequency.

$$M\,(t) = M_0 \left[1 - \frac{7-3\zeta}{2}\frac{k_{\rm e}}{\log_{10}\Lambda_0}\frac{t}{t_{\rm rh,0}}\right]^{\frac{2}{7-3\zeta}} . \qquad (22)$$

We can use this with $k_{\rm e} = 0.3$ to estimate the initial mass and half-mass radius required to give the current values of $M \simeq 2\,500\,{\rm M}_\odot$ and $r_{\rm h} \simeq 2.5\,{\rm pc}$ at $t \simeq 4\,200\,{\rm Myr}$ for M67. However, as Figure 6 shows, a complication arises because ζ as it is defined in eq. (20) is not constant throughout the cluster lifetime. Furthermore, the evolution of a tidally-limited cluster is not self-similar initially.

The initial cluster values can be roughly constrained by the following method. For $M/M_0 \leq 0.5$ the $N = 10\,000$ models show that $\zeta = 5/3$ and $r_{\rm t} = 4r_{\rm h}$. So we choose a value for M_0 and use eq. (17) to find $r_{\rm t,1/2}$, i.e. tidal radius when $M = 0.5M_0$. This defines $r_{\rm h,1/2}$. Next we choose a value for $r_{\rm h,0}$ which can be used with $r_{\rm h,1/2}$ in eq. (20) to calculate an approximate ζ for the $1 > M/M_0 > 0.5$ phase of evolution. Eq. (19) with $N_0 \simeq 2M_0/\,{\rm M}_\odot$ (assuming the average stellar mass at $t = 0.0$ is roughly $0.5\,{\rm M}_\odot$, which is true for the KTG3 IMF) gives $t_{\rm rh,0}$ which we use in eq. (22) to calculate $t_{1/2}$, the time taken for the cluster mass to reduce to half its initial value. From then on the initial parameters in eqs. (20) and (22) can be replaced by the corresponding values at $t_{1/2}$ to find M and $r_{\rm h}$ as a function of time with $\zeta = 5/3$. By iterating on this method we can find the initial values corresponding to current observed cluster properties. It should be noted that the solution is not single-valued: increasing M_0 and decreasing $r_{\rm h,0}$ gives similar values.

There is a problem with this method for M67, demonstrated if we put $M = 2\,500\,{\rm M}_\odot$ in eq. (17) for the standard Galactic tidal field. This gives a tidal radius of 17.5 pc, corresponding to $r_{\rm h} = 4.4\,{\rm pc}$ which is almost twice what is observed. Francic (1989) estimates a lower limit of 9 pc for the tidal radius of M67 and finds no stars with high membership probabilities outside this range. Additionally the data of Fan et al. (1996), from which the current mass is estimated, extend no further than 10 pc from the cluster centre. This agrees well with the observed half-mass radius of 2.5 pc and $r_{\rm t} = 4r_{\rm h}$ from the model data. So does M67 contain less mass than is observed or does its tidal radius not correspond to the standard Galactic tidal field? Chernoff & Weinberg (1990) find that taking $v_{\rm G} = 220\,{\rm km\,s^{-1}}$ for $3 < R_{\rm G} < 20\,{\rm kpc}$ is consistent with current theoretical models of the mass distribution of the Galaxy. The position of M67 relative to the Sun gives $R_{\rm G} \simeq 9\,{\rm kpc}$ so the local tidal field should apply. However, the Galactic orbit of M67 is slightly eccentric (Carraro & Chiosi 1994), with an apogalacticon of 9.09 kpc and a perigalacticon of 6.83 kpc, so it has been subject to a time varying tidal field. Possibly the structure of M67 was altered by an event in its past, such as an interaction with another cluster or an interstellar cloud (Terlevich 1987). We do not dwell on this non-standard tidal radius, preferring to discuss it further in Section 7. What is important is that the mass assumed for M67 corresponds to the observations from which it is derived, i.e. $2\,500\,{\rm M}_\odot$ within 10 pc.

Using this method we estimate that M67 had $N_0 \simeq 40\,000$ and $r_{\rm h,0} \simeq 1\,{\rm pc}$ to evolve to its current observed parameters. This is unfortunate because a simulation with $N_0 > 20\,000$ takes a prohibitively long time with currently available equipment, especially when using a 50% binary fraction. On the other hand the main interest of this work is $N_{\rm BS}$ near 4 200 Myr so it should be possible to extract meaningful results using a semi-direct method.

purpose	escape	escape	escape	M67
N	10 000	10 000	1 000	15 000
t_0 (Myr)	0.0	0.0	0.0	2500.0
distribution model	Plummer	Plummer	Plummer	King, $W_0 = 7$
$r_{\rm h,0}/r_{\rm t,0}$	0.1	0.1[a]	0.03	0.2
$v_{\rm G}$ (km s^{-1})	220	220	220	350
$f_{\rm b}$	0.0	0.11	0.5	0.5
binary separations	EFT30	EFT30	EFT30	EFT10, max 50
#sim	3	3	6	1

[a] 0.06 in one case

Table 3. Model parameters for all simulations described in this work. The final row lists the number of times each simulation was performed. All simulations share the following general properties (see text for details): (i) single star masses taken from KTG3 IMF with minimum and maximum mass limits of 0.1 and $50\,{\rm M}_\odot$; (ii) binary masses taken from KTG1 IMF with a uniform distribution in q; (iii) thermal eccentricity distribution; (iv) $Z = 0.02$; and (v) escape radius of $2r_{\rm t}$.

6 M67 N-BODY MODEL

We start the simulation after the self-similar phase has begun, using an initial model that reflects the preceding stellar, binary and cluster evolution. The model is substantially smaller in population number than the $N \simeq 40\,000$ required to start from the birth of the cluster, so it can be evolved directly to the age of M67 in a reasonable time. In view of the discussion of Section 4 and the small number statistics of the BS population, this is preferable to scaling up the results of a smaller simulation starting from initial conditions. For a first attempt using this method we begin a simulation with $N = 15\,000$ stars at 2 500 Myr. The initial parameters for this semi-direct M67 model and for the simulations from which the escape rates were derived (see previous Section) are summarized in Table 3.

To estimate the binary fraction and the maximum orbital separation for the binaries in this starting model we consider the hard binary limit for the cluster. If indeed $N_0 = 40\,000$ and $r_{\rm h,0} = 1\,{\rm pc}$ then $a_{\rm hard} \simeq 10\,{\rm AU}$ for M67 initially, whereas it is now more like 140 AU. Only binaries which were initially hard could survive the early phases of cluster evolution so a conservative estimate of 50 AU is used for the upper limit of the separation distribution in the starting model. Lowering this limit would increase the incidence of interaction within binary systems and presumably lead to a larger number of BSs produced by the simulation. This would not be accompanied by an increase in the number of BSs found in wide eccentric orbits as the population of wide binaries available for exchange interactions is decreased. As already mentioned, observations of M67 indicate that the current binary fraction could be as high as 50%. During the cluster evolution soft binaries are broken-up in dynamical

lower mass	upper mass	number fraction	mass in single stars	mass in binaries
0.100	0.137	0.081	94.8	0.0
0.138	0.190	0.089	144.7	0.0
0.191	0.263	0.097	170.5	50.4
0.264	0.363	0.105	199.5	124.3
0.364	0.502	0.107	220.7	236.9
0.503	0.694	0.193	362.3	785.6
0.695	0.960	0.148	378.3	827.6
0.961	1.326	0.116	272.1	1038.1
1.327	1.833	0.055	118.6	732.5
1.834	2.532	0.005	16.9	83.6
2.533	3.500	0.004	0.0	98.6

Table 4. Mass groups used to populate the M67 starting model. All masses are in units of $M_\odot$. The lower and upper mass limits of each group are given in the first two columns, followed by the number fraction of stars in that group for the combined $N = 10\,000$ with $f_b = 0.11$ models at 2 500 Myr. 5 000 single stars and 5 000 binaries, all evolved to an age of 2 500 Myr (see text for details), are chosen for the M67 starting model according to these number fractions. The resulting masses in single stars and in binaries for each mass group in the M67 starting model are given in the final two columns.

encounters so this is a lower limit on the primordial fraction. However, hard binaries are retained preferentially by the cluster because they have a higher average mass than single stars. We therefore assume that the binary fraction has remained roughly constant during the cluster lifetime, in good agreement with the $N = 10\,000$ data, so we use $f_b = 0.5$ for the starting model.

We use results from the previous simulations to estimate what the mass function (MF) will look like at 2 500 Myr. Figure 7 shows the IMF for the $N = 10\,000$ models that included binaries and the corresponding MF for the population at 2 500 Myr according to the population synthesis code and from the N-body simulations at the same age. It is evident that dynamics and the tidal field alter the MF, lowering it at the low-mass end and increasing the relative number of more massive stars. The number of BSs produced will be sensitive to the shape of the MF assumed for the starting model as a larger proportion of systems with mass comparable to that of the MS turn-off at a particular time will lead to more stragglers at that time. To generate the starting population for the semi-direct M67 simulation, we evolve a large population with a 50% binary fraction and $Z = 0.02$ to an age of 2 500 Myr using the population synthesis code alone. The single star masses are chosen from the KTG3 IMF and the binary masses and parameters are chosen in the same way as for the population synthesis run PS6, but with an upper limit of 50 AU in the separation distribution. Then using the information gained from the dynamically altered MF in Figure 7, i.e. the ratio of stars in each mass bin between the dynamical and non-dynamical MFs, we take 5 000 single stars and 5 000 binaries from the large population to populate the starting model (see Table 4). This gives a starting mass of 6 000 $M_\odot$ for the cluster at 2 500 Myr.

We use a tidal field with $v_G = 350\,\mathrm{km\,s^{-1}}$ at $R_G = 8.5$ kpc which fixes $r_t = 17$ pc. This tidal radius determines the length scale used in the N-body simulation. The stars

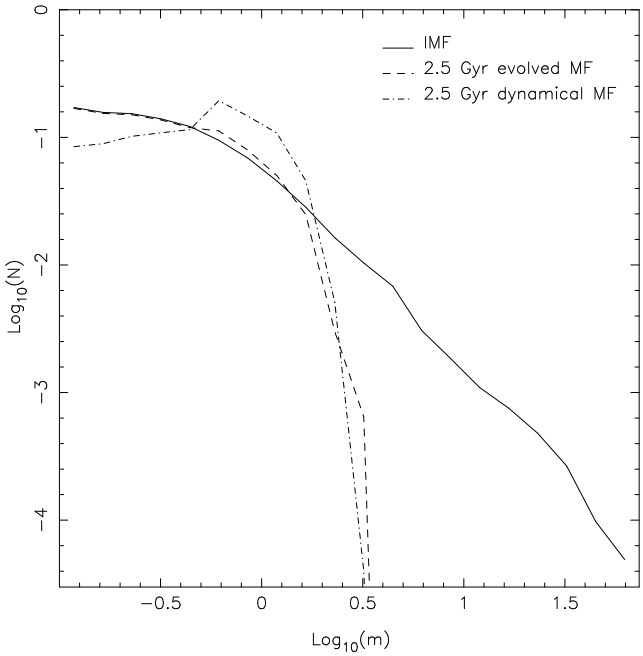

Figure 7. The full line shows the normalized IMF for a population with 11% binaries where the single star masses are chosen from the KTG3 IMF and the binary masses from the KTG1 IMF. The dashed line shows the mass function (MF) of the same population evolved to 2 500 Myr (note this is hidden by the full line for $\log m/\,M_\odot < -0.35$) and the dash-dot line shows the MF of the same population evolved to 2 500 Myr in the N-body code with a standard tidal field.

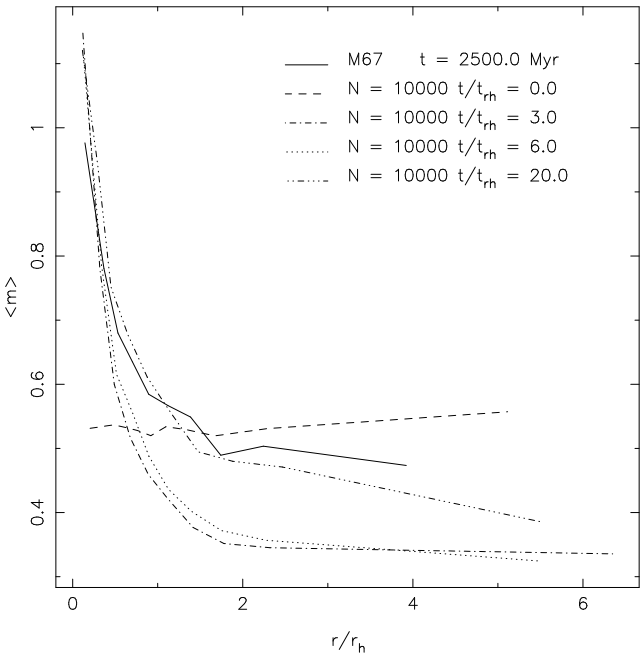

Figure 8. Profile of the average stellar mass in successive Lagrangian shells. The radius is scaled by the cluster half-mass radius. Each Lagrangian shell contains 10% of the cluster mass. The profiles plotted are for the combined $N = 10\,000$ models data at $t/t_{rh} = 0.0$, 3.0 (near core-collapse), 6.0 (when the model has lost half its mass) and 20.0, as well as for the initial M67 model at 2 500 Myr.

are distributed according to a multi-mass King model (King 1966; Chernoff & Weinberg 1990) with $W_0 = 7$ and a central number density $n_0 = 2.28 \times 10^3\,\mathrm{pc}^{-3}$. The concentration of the model is determined by the dimensionless parameter

$$W_0 = \frac{\Psi_0}{\sigma^2}\,, \tag{23}$$

where Ψ_0 is the central potential and we use a central velocity dispersion $\sigma^2 = 3 \times 10^{10}\,\mathrm{cm}^2\,\mathrm{s}^{-2}$. These positions are scaled so that the cluster just fills the tidal radius, which results in a half-mass radius of 3.4 pc for the starting model. Figure 8 shows the evolution of the average stellar mass profile for the combined $N = 10\,000$ model data. It can be seen that as the models evolve, two-body effects cause the heavier stars to segregate towards the inner regions. Using the King model to determine the initial spatial distribution of the stars for the M67 simulation builds in a degree of mass-segregation so that this energy equipartition is taken into account.

We can estimate the relation between the mass of our starting model and its mass at 4 200 Myr using the escape rates discussed in Section 5, but this depends on how binaries contribute to the value of N used in the calculation. If we assume that relatively hard binaries act as single stars when modelling relaxation effects then N would be 10 000 and the mass at 4 200 Myr should be about $1\,500\,\mathrm{M}_\odot$. On the other hand, if the binary components behave as single stars then $N = 15\,000$ and the mass left would be about $3\,000\,\mathrm{M}_\odot$. Either way this is close enough to the mass derived from observations to proceed with the simulation.

We evolve the model to $T = 4\,310$ Myr using `NBODY4`. At this time the cluster mass is $1\,140\,\mathrm{M}_\odot$. It consists of 560 single stars and 740 binaries, the tidal radius is 10 pc and the half-mass radius is 2.5 pc. The mass in single stars and binaries with masses greater than $0.5\,\mathrm{M}_\odot$ is $1\,050\,\mathrm{M}_\odot$, more than 90% of the total mass. The simulation lasted for 1 260 N-body time units and took one month dedicated use of the HARP-3.

Figure 9 shows the evolution of the number of BSs present in the simulation. Also shown are the numbers of triple systems, RS CVn systems and binaries containing a BS. At $T = 4\,200$ Myr there are 22 BSs in the model but only one of these is in a binary. There is only one RS CVn system in the cluster at this time. The highest number of BSs present at any one time is 29 at $T = 3\,653$ Myr with seven of these in binaries. At this time there are three RS CVn systems.

Shown in Figure 10 is the period-eccentricity distribution of all BS binaries formed during the simulation. Of these, five are BS-BS systems. There appears to be two fairly distinct BS binary populations, one consisting of close circular orbits and the other with wider eccentric orbits. The BSs in circular orbits formed by stable mass-transfer, beginning in general when the primary is in the Hertzsprung gap (HG). These still have their primordial companion which evolves to become a WD. No instance of a BS formed from Case C mass transfer, or as a result of wind accretion, occurs in this simulation. For the relatively wide binaries, $P > 100$ d, the distribution appears uniform for $e > 0.2$. These binaries form in hierarchical systems or as a result of an exchange interaction. A star is more likely to be exchanged into a wide orbit than into an existing hard binary. We also expect that

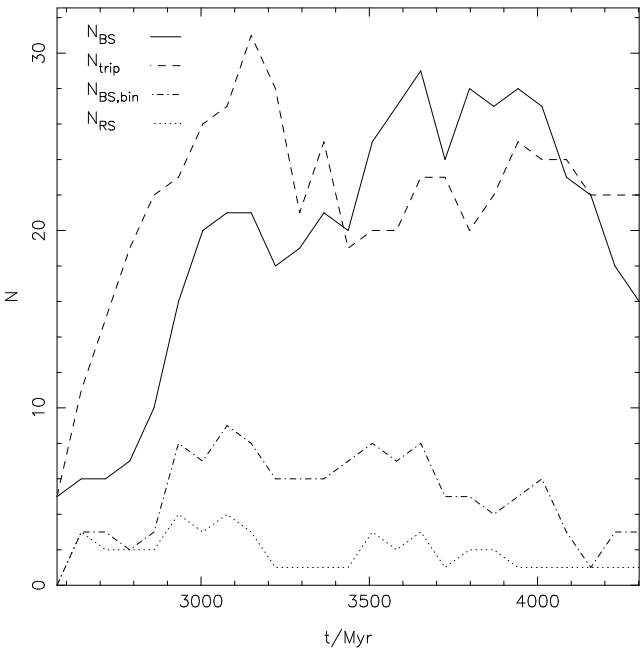

Figure 9. The evolution of the number of blue stragglers (full line), triple systems (dashed line), blue straggler binaries (dash-dot line), and RS CVn systems (dotted line), in the M67 simulation.

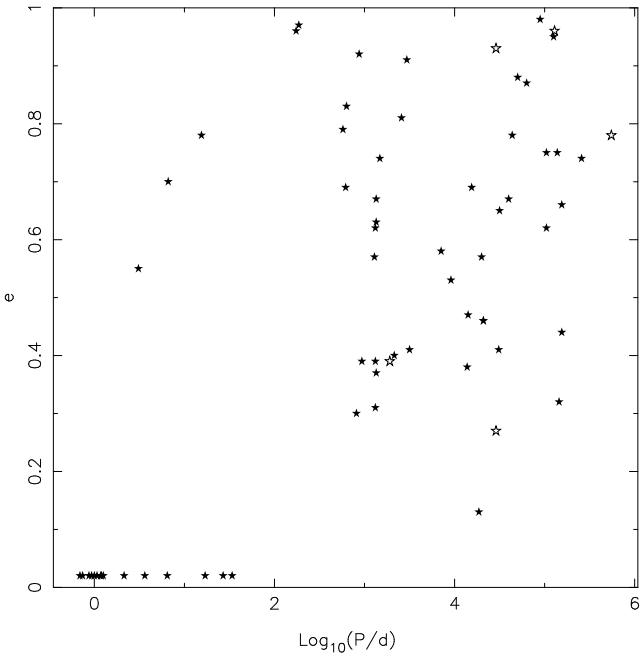

Figure 10. Distribution of periods and eccentricities for binaries formed with a blue straggler component during the M67 simulation. The open points represent BS-BS binaries, i.e. each component is a BS.

the eccentricities of newly formed binaries follow a thermal distribution (Heggie 1975), which is proportional to the eccentricity. Furthermore, since exchange interactions tend to take place in the dense central regions of the cluster it is not surprising to find a paucity of wide circular binaries. A total of 53 exchange interactions were recorded during

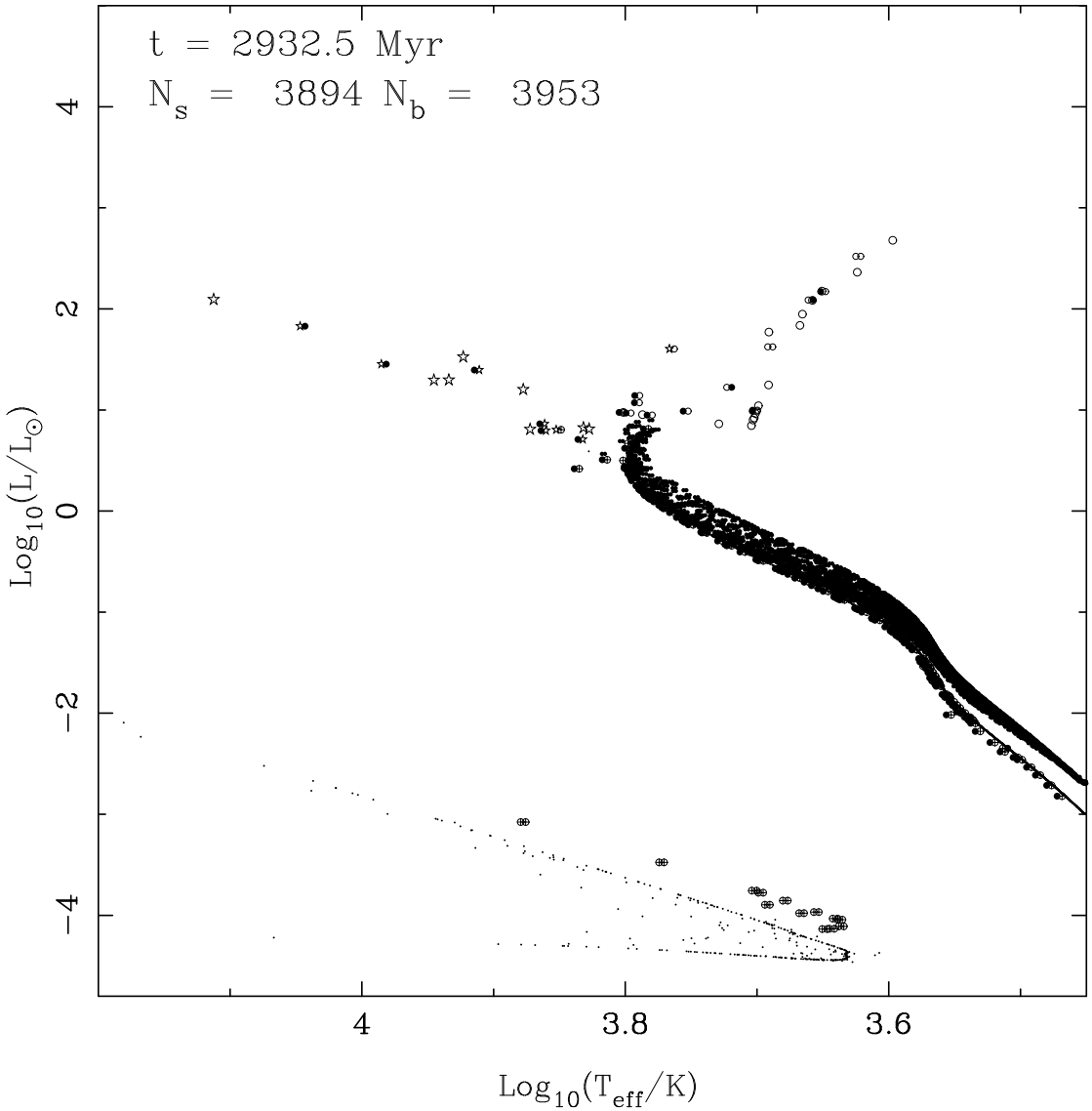

Figure 11. Hertzsprung-Russell diagram for the M67 N-body simulation at an age of 2 932.5 Myr when 3 894 single stars and 3 953 binaries remain. Main-sequence stars (dots), blue stragglers (open stars), sub-giants, giants and naked helium stars (open circles) and white dwarfs (dots) are distinguished. Binary stars are denoted by overlapping symbols appropriate to the stellar type of the components, with main-sequence binary components depicted with filled circles and white dwarf binary components as $\oplus$ symbols. The effective temperature of a binary is computed according to Hurley & Tout (1998).

the simulation. Of these, 18 are the result of a direct exchange and the remaining 35 are the result of 12 resonant exchanges (Heggie 1975). In a resonant exchange the three (or four) stars involved in the interaction form a temporary bound system which can then undergo a series of exchanges in quick succession before one (or two) of the stars escapes.

On average half the BSs formed during the simulation would have done so without the introduction of cluster dynamics. We note however that the cluster environment was taken into account when choosing the binary parameters for the starting model, effectively doubling the number of BSs expected when compared with population synthesis run PS6. Consider the 16 BSs present when the simulation ended, of which three are in binaries. Seven of these formed from standard Case A mass transfer in a primordial binary: the two components coalesced to leave a single BS. One formed as a result of standard Case B mass transfer and is in a circular orbit with a 17 d period with its original companion, now a WD. Another two formed from Case A mass transfer but only after a series of close encounters had altered the orbital parameters and caused each system to circularize. Without perturbations to their orbits these stars would not have been close enough to interact. The remaining BSs are the result of collisions within binary systems, three after a star was exchanged into a highly eccentric orbit and the other three after perturbations to the existing binary increased the eccentricity and caused the orbit to become chaotic. One of the BS binaries that formed from a dynamical interaction has a period of 813 d and $e = 0.3$ and the other has $P = 6.6$ d and $e = 0.7$. The BS in the wider of these has a mass $M_1 = 1.6\,\mathrm{M}_\odot$ and was created after Case A mass transfer in a primordial binary lead to coalescence. Later in

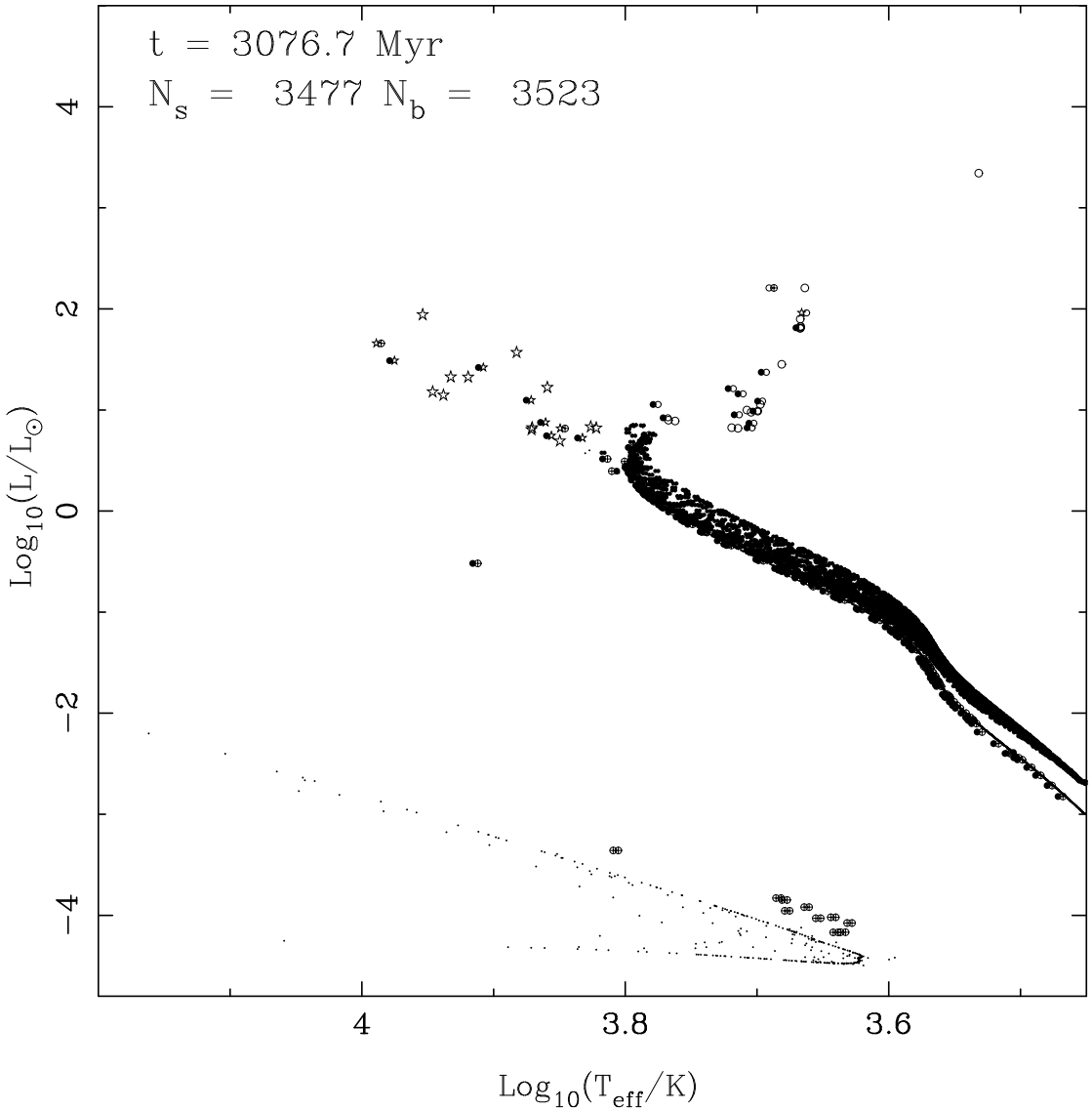

Figure 12. As Figure 11 at 3 076.7 Myr. Present in the cluster at this time are 21 blue stragglers, nine of which are in binaries. One GB star has a BS binary companion in an eccentric orbit. A CHeB star and a WD in an eccentric binary is also present. There are ten cataclysmic variables and ten double-degenerate systems.

the cluster evolution it underwent an exchange interaction with a wide binary to form the existing binary. The companion is a MS star with $M_2 = 1.3\,\mathrm{M}_\odot$ and the star that left the temporary three-body system was the lightest of the three, $M_3 = 0.7\,\mathrm{M}_\odot$. The other binary was originally part of a three-body hierarchy consisting of an outer component in an eccentric orbit about a primordial binary with $P = 301$ d and $e = 0.18$. Inclination-induced perturbations drove the inner eccentricity up to 0.94 at which point one of the inner MS components collided with the third MS star, producing the BS, which remains bound to its original companion.

Figures 11, 12, 13, 14, 15 and 16 show the Hertzsprung-Russell diagram of the cluster model at various epochs. The spatial distribution at 2 933 Myr and at 4 302 Myr is shown in Figures 17 and 18 respectively, as the cumulative radial profiles in XY- and YZ-planes[§]. It is evident that the BSs are concentrated towards the core of the cluster.

At $T = 4\,014$ Myr (Figure 15) there are two super-BSs in the cluster. One of these has a mass 2.3 times the then turn-off mass of $1.32\,\mathrm{M}_\odot$. The other has a mass of $2.7 M_{\mathrm{TO}}$ and is in a binary with another BS. A total of eight super-BSs formed during the simulation. Also present in the cluster at $T = 4\,014$ Myr are nine cataclysmic variables and three double-degenerate systems. There are 19 giants, six of which are in binaries. One of the 27 BSs is in a binary with an AGB star separated by 4×10^{-4} pc. This is about $0.1''$ at the distance of M67, so it would not appear as a BS on a cluster CMD (the CCD used by MMJ had $0.77''$/pixel).

[§] Full colour versions of the Hertzsprung-Russell diagrams and the spatial distributions, at a larger number of epochs, can be found at www.ast.cam.ac.uk/∼cat/m67.html.

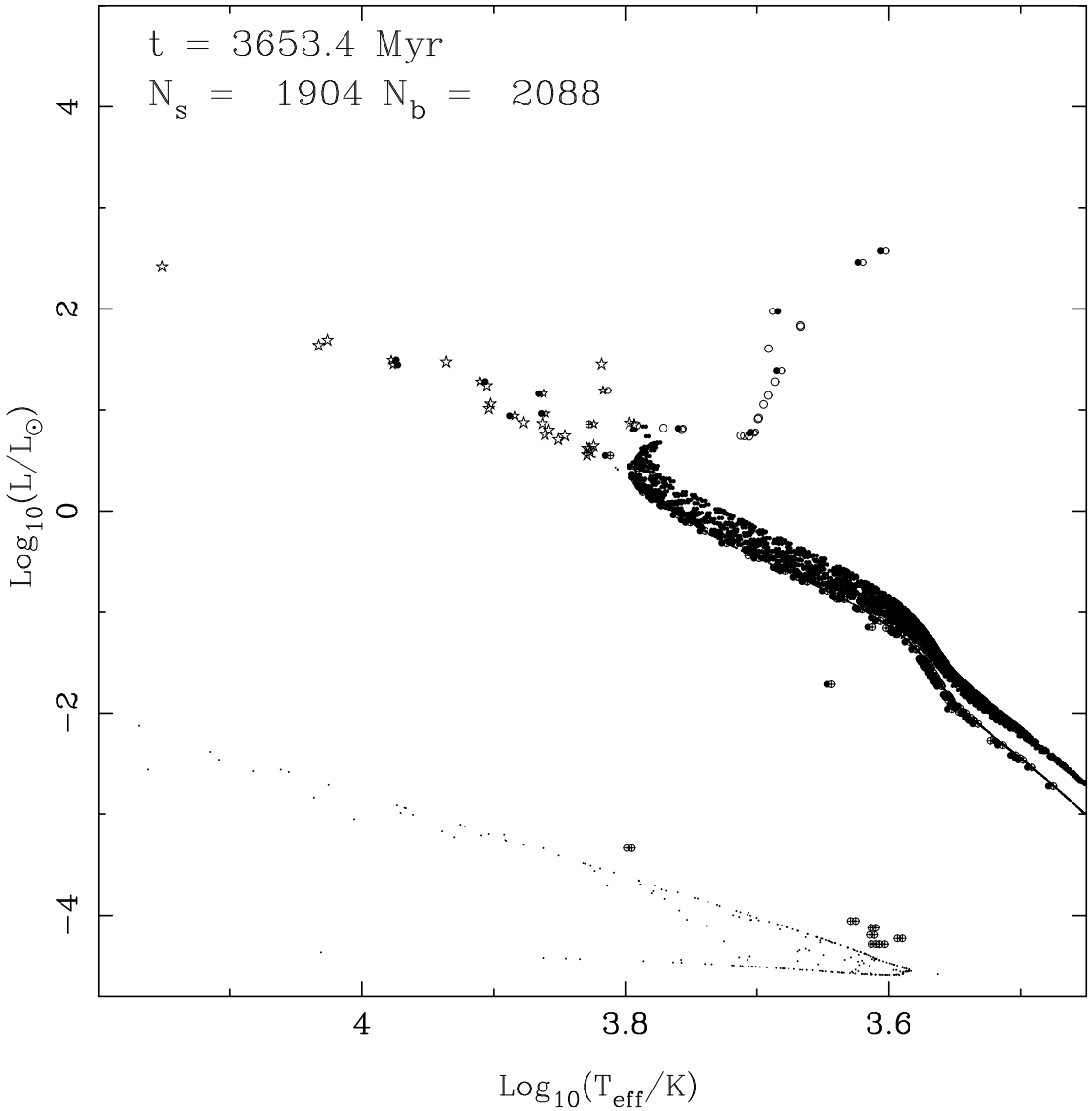

Figure 13. As Figure 11 at 3 653.4 Myr. Present in the cluster at this time are 29 blue stragglers, the maximum number during the simulation, with eight of these in binaries. There is one super-BS, five cataclysmic variables and seven double-degenerate systems. The depletion of double-degenerate systems is due to ejection of some close systems and break-up of some wide systems.

The $2.7M_{\rm TO}$ super-BS in the model at 4 014 Myr is an interesting case. At the beginning of the simulation it is a single star with mass $M_1 = 1.33\,{\rm M}_\odot$. At 3 190 Myr it enters a triple system in which it exchanges into the original binary. The resulting binary has orbital parameters $P = 9\,120\,{\rm d}$ and $e = 0.52$ and survives to 3 740 Myr when it is involved in a binary-binary encounter. This leaves the proto-BS in an orbit of $P = 153\,{\rm d}$ and $e = 0.99$ with a companion of mass $M_2 = 1.0\,{\rm M}_\odot$. Owing to the large eccentricity the binary components collide and merge to form a BS of mass $M_1 = 2.33\,{\rm M}_\odot$. At 3 870 Myr this BS is involved in a three-body interaction and forms another binary, this time with a star of mass $M_2 = 2.28\,{\rm M}_\odot$ which is itself a BS. The BS-BS binary has $P = 1\,350\,{\rm d}$ and $e = 0.67$. At 3 990 Myr this binary forms a stable four-body hierarchy with yet another binary, the original BS collides with one of the stars in the other binary, forms the super-BS with $M_1 = 3.45\,{\rm M}_\odot$, and remains bound to the other BS. The fourth body escapes and leaves the binary that is observed at 4 014 Myr. Later at 4 080 Myr the super-BS and BS collide when the eccentricity of the orbit has grown to 0.93 as a result of external perturbations. This makes a BS with $M_1 = 5.7\,{\rm M}_\odot$, i.e. $4.4M_{\rm TO}$. The new super-BS captures a companion at 4 112 Myr, with which it then collides to form a super-BS with $M_1 = 7.7\,{\rm M}_\odot \simeq 6M_{\rm TO}$. Soon after it strongly interacts with a hard binary and gets ejected from the cluster.

7 DISCUSSION

An obvious problem with our M67 model is the lack of BSs in wide circular binaries because two such systems, S975 and S1195, are observed in the real cluster. Leonard (1996) suggests these may be the result of mass transfer from a core helium-burning (CHeB) primary star. This does not seem likely because a star does not get any bigger during

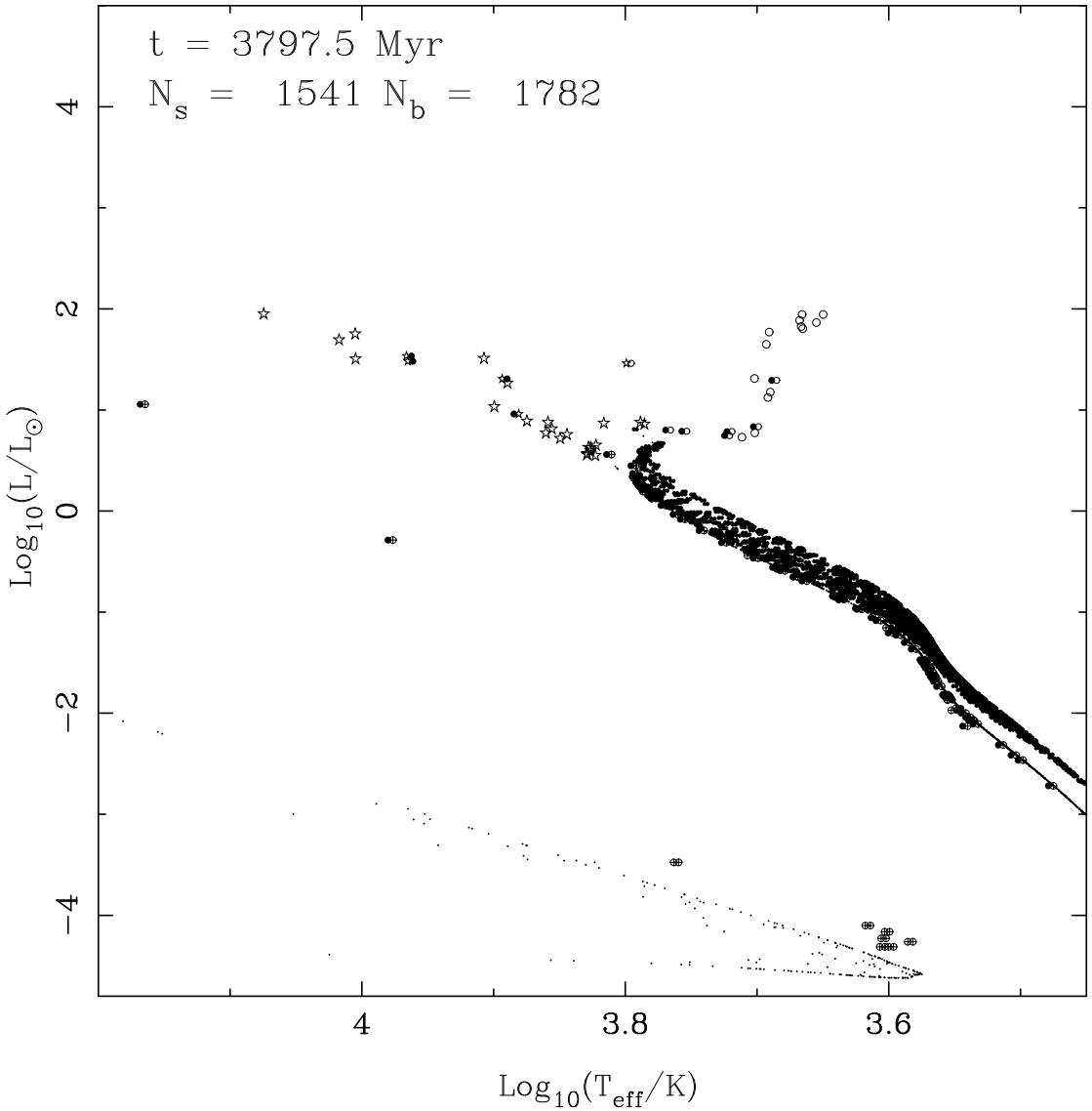

Figure 14. As Figure 11 at 3 797.5 Myr. Present in the cluster at this time are 28 blue stragglers with five of these in binaries. One BS binary has a GB star companion which is currently filling its Roche-lobe and transferring mass. There is one super-BS, seven cataclysmic variables and seven double-degenerate systems.

CHeB than it did on the GB, so if the primary does not fill its Roche-lobe on the GB, i.e. Case B mass transfer, Case C mass transfer is very unlikely before the star has reached the AGB. If mass transfer does occur when the primary is on the AGB then common-envelope evolution can only be avoided if the primary has lost enough of its envelope to become the less massive star. Wide binaries can form via exchange in the cluster but the results show this is unlikely to produce circular orbits. So it would seem that a number of wide circular BS binaries should be formed by isolated evolutionary processes, either from stable Case C mass transfer or wind accretion. However, hardly any such binaries are produced with the period distributions used in the population synthesis runs. Perhaps this indicates that a bi-modal period distribution is required, or that the peak in the distribution should cover a wider range of periods. A more likely solution is that the wind-accretion efficiency we have used is too low. Our treatment of wind accretion in the binary evolution model assumes that the wind velocity $V_{\rm W}$ is simply $V_{\rm esc}/\sqrt{2}$ where $V_{\rm esc}$ is the escape velocity from the surface of the star (see Section 2.1 of Hurley, Tout & Pols 2000 with $\beta = 0.5$). The accretion rate is approximately proportional to $V_{\rm W}^{-4}$ so that a small error in $V_{\rm W}$ has a large effect. We repeated run PS6 with the wind velocity reduced by a factor of 2, i.e. $\beta = 1/8$ in Section 2.1 of Hurley, Tout & Pols (2000). This is actually more in keeping with observations. The result is $N_{\rm BS} = 5.1$ and $N_{\rm RS} = 4.3$ at 4.2 Gyr with 23% of the BSs in close binaries and 16% in wide binaries ($P > 1$ yr). The average period of these wide BS binaries is 2 000 d which is consistent with the M67 BS binaries. In future N-body simulations we will incorporate this variation. Furthermore, if we use the weaker criterion of Webbink (1988) to determine the onset of dynamical mass transfer at RLOF (see Section 2.6.1 of Hurley, Tout & Pols 2000), an additional channel for the formation of binary BSs is created. Repeating run PS6 with $q_{\rm crit}$ according to Webbink (1988), together with $\beta = 1/8$,

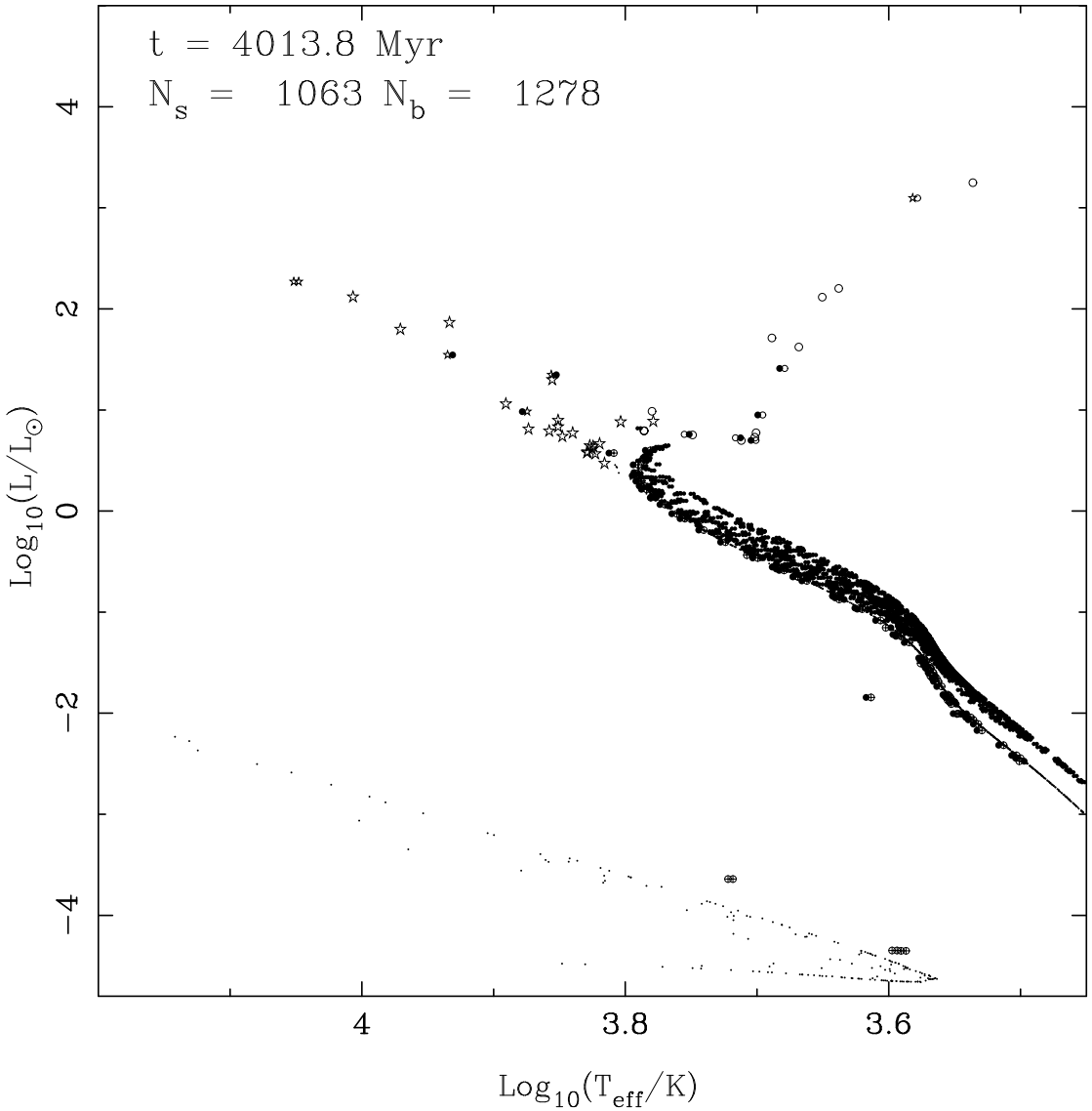

Figure 15. As Figure 11 at 4 013.8 Myr. Present in the cluster at this time are 27 blue stragglers with six of these in binaries. There are two super-BSs and one BS-BS binary. There are nine cataclysmic variables and three double-degenerate systems.

gives $N_{\rm BS} = 5.5$ at 4.2 Gyr with 22% of the BSs in close binaries and 22% in wide binaries.

None of the eccentric BS binaries in the model are the result of stable mass transfer followed by perturbations to the circular orbit. Primarily this is because no BSs are formed in wide circular binaries in the first place, but even if they were the eccentricity induced would be small and tidal forces would quickly return the orbit to circularity. Rasio & Heggie (1995) show that the induced eccentricity $e_{\rm f}$ varies as

$$e_{\rm f} \propto \left(\frac{r_{\rm p}}{a}\right)^{-5/2}, \qquad (24)$$

where $r_{\rm p}$ is the separation at periastron. Therefore an eccentric orbit is more likely to be altered by a close encounter. Assuming a stellar number density of $20\,{\rm pc}^{-3}$ and a velocity dispersion of $0.40\,{\rm km\,s}^{-1}$ in the core of M67, Leonard (1996) uses the result of Rasio & Heggie (1995) to derive a mean induced eccentricity of $e \simeq 10^{-3}$ for wide, $P = 10^4$ d, circular orbits.

Not surprisingly most of the eccentric BS binaries are the result of exchange interactions and none are produced from tidal capture. The exchange timescale can be expressed as

$$\tau_{\rm ex} = \frac{1}{n_{\rm b}\,\Sigma\,V_{\rm rel}}, \qquad (25)$$

where $n_{\rm b}$ is the binary number density, $V_{\rm rel}$ is the relative speed of the third body and the binary centre-of-mass, and Σ is the exchange cross-section. Consider the likelihood of a BS of mass $M_3 = 2.0\,{\rm M}_\odot$ being exchanged into a binary with $M_1 = 1.0\,{\rm M}_\odot$ and $M_2 = 0.5\,{\rm M}_\odot$. From the results of binary-single-star scattering experiments performed by Heggie, Hut & McMillan (1996) the exchange cross-section to displace M_1 is $13\,300\,a\,{\rm AU}^2$ and to replace M_2 is $35\,400\,a\,{\rm AU}^2$. Taking $n_{\rm b} = 20\,{\rm pc}^{-3}$, $V_{\rm rel} = 1\,{\rm km\,s}^{-1}$ and $a = 100$ AU gives $\tau_{\rm ex} \simeq 540$ Myr which is an order of magnitude less than the age

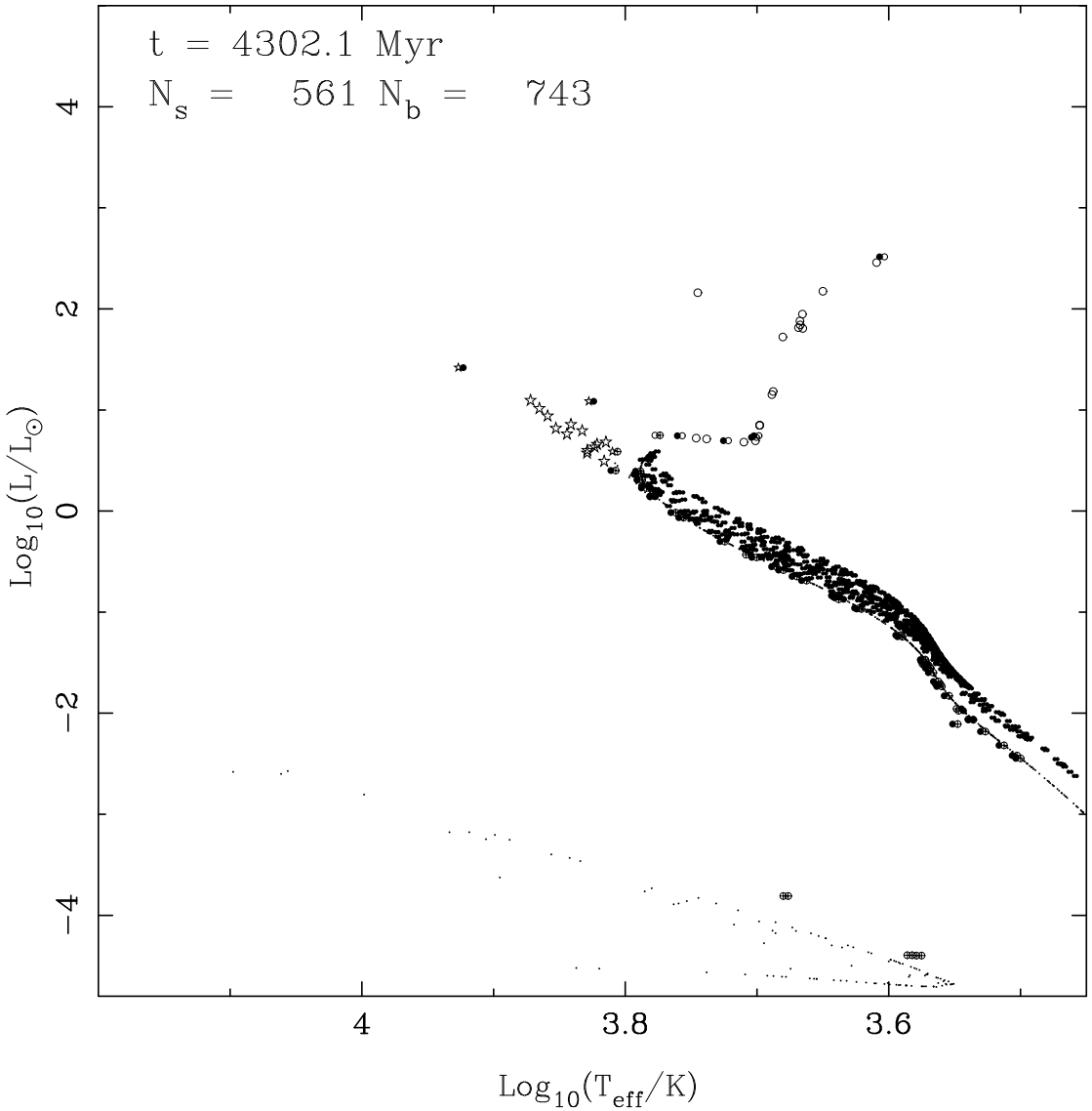

Figure 16. As Figure 11 at 4 302.1 Myr (the end of the simulation). Present in the cluster at this time are 16 blue stragglers with three of these in binaries. There are six cataclysmic variables and three double-degenerate systems.

of M67. On the other hand, the tidal capture timescale for the BS is about 10^4 Myr (Press & Teukolsky 1977). This is confirmed by Portegies Zwart et al. (1997) who find that in a cluster core with $\log\left(n/\mathrm{pc}^{-3}\right) = 3.92$ the low encounter rate means that tidal capture is rare. We must however be careful with the definition of tidal capture because some BS binaries in the M67 model do form from bound triple systems which themselves formed from a binary-single-star interaction.

Even though during the M67 simulation two BSs, formed from a collision within a triple system, are found in short-period eccentric orbits it is hard to see how the cluster dynamics can produce significant numbers of these binaries. The exchange cross-section is proportional to the binary separation (Heggie, Hut & McMillan 1996) so they are unlikely to be formed in this way (see Figure 10). Allowing for the chance formation of a tidal capture binary, the calculations of Portegies Zwart et al. (1997) show that capture binaries in a dense cluster core are generally close with $a < 10\,\mathrm{R}_\odot$ but that 60% of these circularize during the formation process. So for every BS observed in a close eccentric orbit at least one should be found in a close circular orbit. BSs in close circular orbits can be formed from Case B mass transfer but these are even less likely to have an eccentricity induced than wide circular binaries. A possibility that has yet to be considered and does not rely on cluster dynamics is formation via common-envelope evolution when unstable Case B mass transfer occurs. The processes involved in common-envelope evolution are very uncertain (Iben & Livio 1993) and there is no real reason to assume that a binary emerging from this phase should be circular. Therefore the binary S1284 observed in M67 could be produced in this way or possibly by a collision within a triple system.

The number of blue stragglers produced by the M67 model is in good agreement with the observations. Figure 1

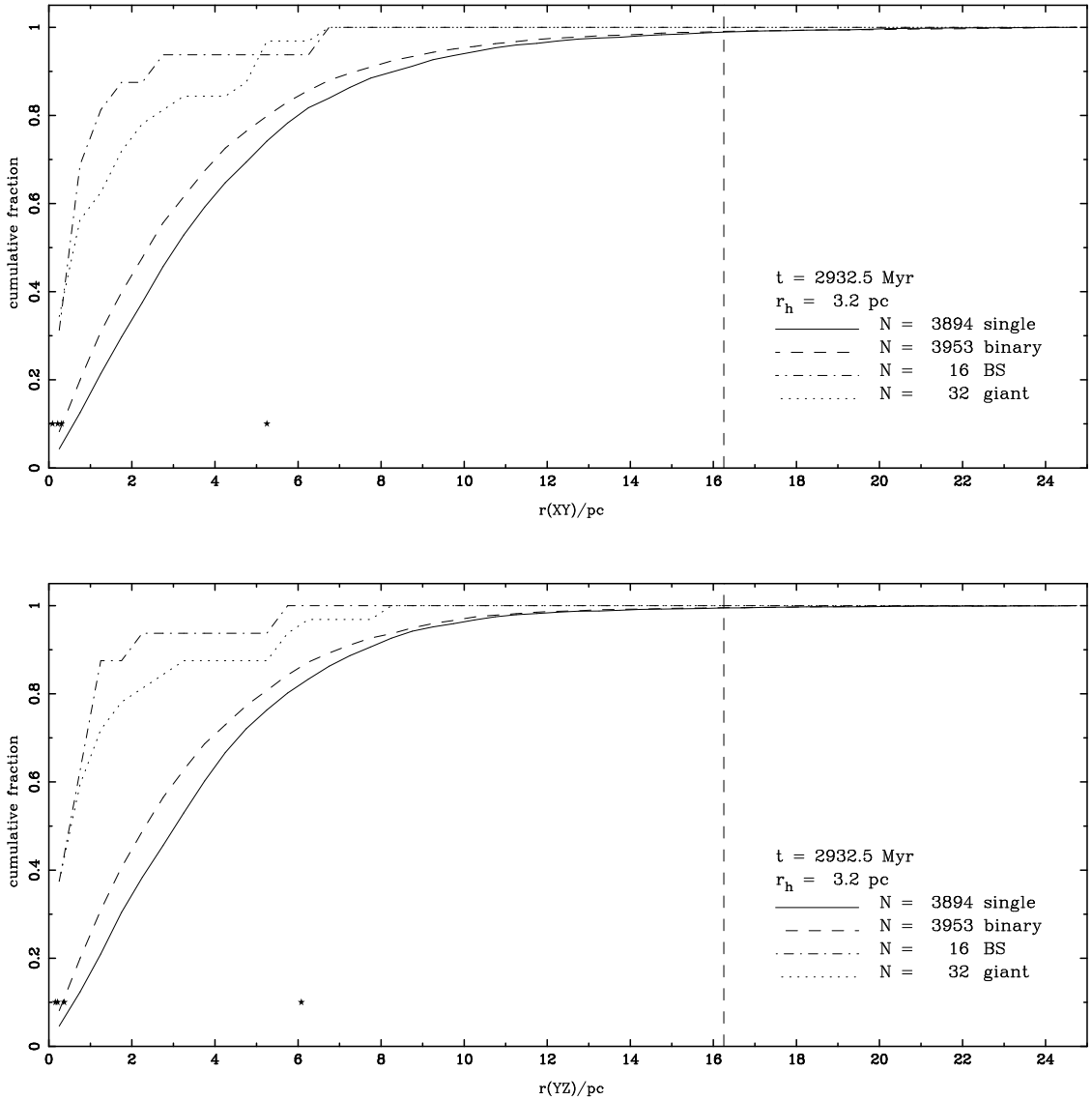

Figure 17. Cumulative radial profiles in the XY- and YZ-planes for the population shown in Figure 11. The tidal radius is 16.3 pc (vertical dashed line), the half-mass radius is 3.2 pc and the half-mass radius of the blue straggler stars is 0.8 pc. Note that stars are not actually removed from the simulation until they are at a distance greater than two tidal radii from the cluster centre. Both blue stragglers and giants congregate towards the centre. The four RS CVn systems present are plotted as filled stars.

shows that the cluster environment is very effective at increasing the relative number of the BS population. If it had been possible to start a full simulation from $T = 0$ then hopefully the relative number of BSs would increase gradually with time to reach the M67 point, rather than the rapid increase produced by the semi-direct simulation (although the log-scale in Figure 1 distorts the actual range of the simulation). As expected the BSs formed by a variety of paths, Case A and Case B mass transfer in binaries with orbital parameters unaffected by the cluster environment, Case A mass transfer after perturbation-induced circularization, and collisions in highly eccentric binaries.

In population synthesis without cluster dynamics the dominant formation mechanism is Case A mass transfer. However, Mathys (1991) has observed that M67 BSs rotate slower than average for MS stars. As noted by Leonard & Linnell (1992), tidal synchronization in a close binary should cause BSs produced by Case A mass transfer to be rapid rotators. Magnetic braking will not be effective at reducing the rotation rate because MS stars with $M \gtrsim 1.3\,\mathrm{M}_\odot$ do not have convective envelopes. It is uncertain whether BSs resulting from collisions between two MS stars will be rapid rotators but it is interesting that 50% of the BSs in the N-body model came from direct collisions in eccentric binaries. The progenitor stars will not have been affected by standard tidal circularization in this case but it is unclear what the effect of any angular momentum exchange during chaotic motions of the orbit will have on the stellar spins. Our simulation did not form any BSs from hyperbolic collisions between two single stars, in agreement with the collision timescale predicted by Press & Teukolsky (1977), which is about 10^6 Myr for a $1\,\mathrm{M}_\odot$ star in the core of M67.

An encouraging number of wide eccentric BS binaries are formed during our simulation. Super-BSs are also made,

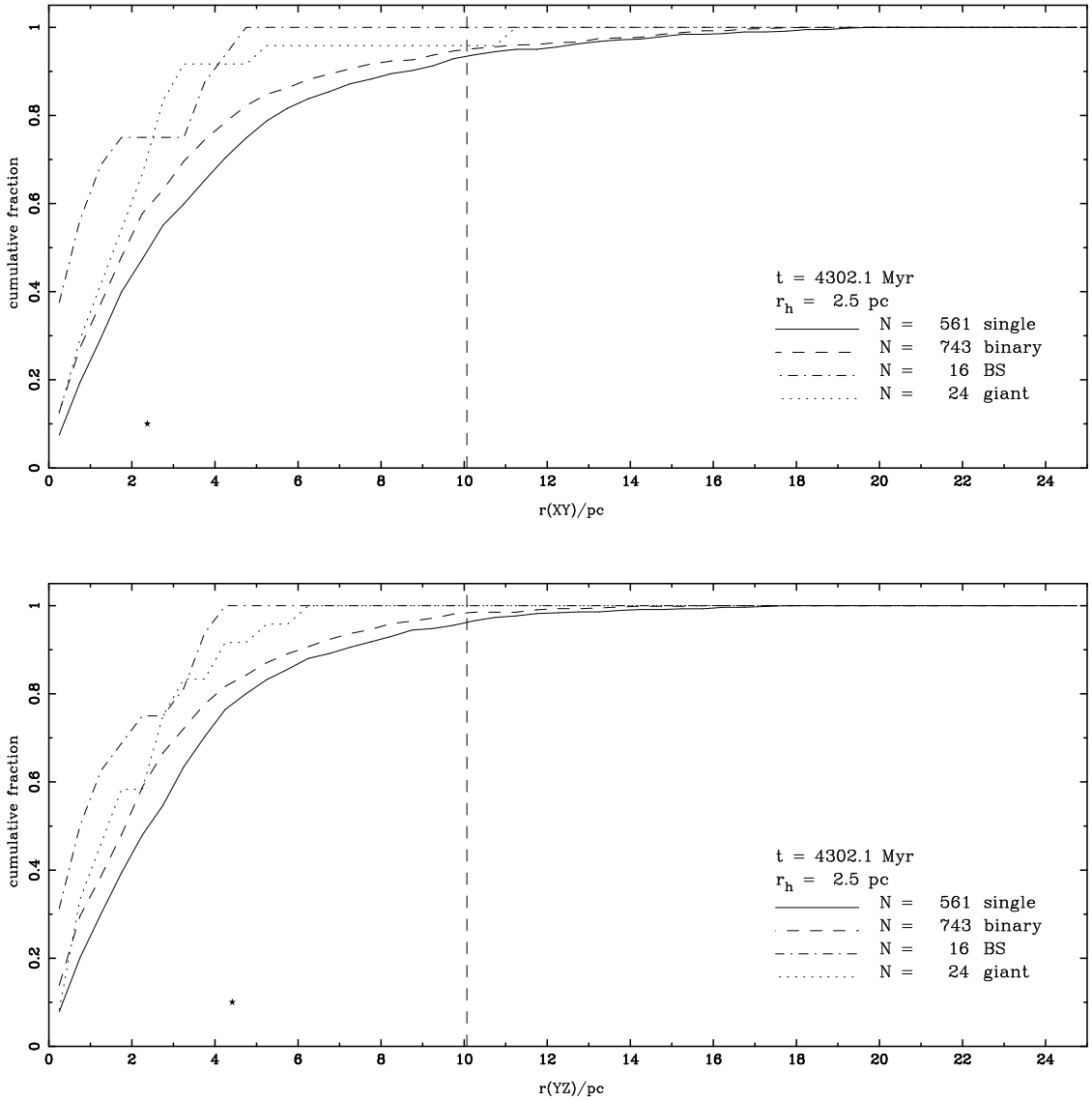

Figure 18. Cumulative radial profiles in the XY- and YZ-planes for the population shown in Figure 16. The tidal radius is 10.1 pc (vertical dashed line) and the blue straggler half-mass radius is 0.9 pc. The RS CVn system present is plotted as a filled star.

as well as some short period binary BSs in eccentric and circular orbits. So the model contains formation paths for all the BSs observed in M67, except wide circular BS binaries but this can be rectified as discussed above. Another discrepancy is that the frequency of model BSs found in binaries is too low. The BS half-mass radius in the model is smaller than the half-mass radius of the MS stars, in qualitative agreement with the observations, but is itself a factor of 2 less than is observed for M67. Also too many potential RS CVn systems are broken-up in the cluster core which suggests that the population within the half-mass radius is too centrally condensed. Observations of M67 suggest that the number density of stars is about $n = 40\,\mathrm{pc}^{-3}$ within a core of radius 1 pc, while the model at 4 300 Myr has $n = 150\,\mathrm{pc}^{-3}$ within 1 pc of the cluster centre and $n = 34\,\mathrm{pc}^{-3}$ inside the half-mass radius. A decrease in the central concentration implies that wide binaries formed from exchange interactions have longer lifetimes.

The use of a rather unusual tidal field in the M67 model, prompted by the observed boundary of 10 pc for the cluster stars, deserves further discussion. Preferential escape of low-mass stars from the model owing to two-body encounters shows that the current observed mass of M67, for stars with masses greater than $0.5\,\mathrm{M}_\odot$, may be close to the actual cluster mass, and therefore a standard tidal field may well apply. The case for this is strengthened when we consider that the observed boundary of the cluster members is only a lower limit for the tidal radius. However, it is interesting that $v_\mathrm{G} = 350\,\mathrm{km\,s}^{-1}$ is not ruled out by the model of the Milky Way halo presented by Wilkinson & Evans (1999). Additionally, Baumgardt (1998) has shown that it is the tidal radius at perigalacticon of an eccentric orbit that determines the dissolution of a star cluster. The main effect of a stronger tidal field is to drive the cluster evolution at a higher rate. Therefore it is possible that use of a standard tidal field would cause the peak in N_BS that we see in Figure 9 to

occur at a later time, closer to the age of M67. It is also possible that as the core would not be as dynamically evolved it would be less dense, leading to a greater population of wide binaries and RS CVn systems. We should stress that these points are purely conjecture and that the tidal field requires close attention in future simulations. In particular, work is currently underway to implement a time-varying tidal field in `NBODY4` which will enable eccentric cluster orbits to be followed (Wilkinson & Hurley 2001).

Ideally it would be desirable to perform more simulations and investigate the effects of varying parameters such as the central concentration in the starting model. Many factors are uncertain, both in the model and the observations. For example, the derived escape rate may not be correct for larger N so the size of the starting model, in terms of both star number and length scale, may not be relevant to the conditions of M67 at birth. In all of this it would be helpful if we could begin a complete simulation from initial conditions but, considering that a single semi-direct simulation took a month to perform, the capability of the current hardware is already pushed to its limit. Future improvements in computing efficiency, such as the availability of GRAPE-6 (Makino 1999), will enable a leap forward in the field of star cluster modelling. The ability to perform direct simulations of clusters like M67 comfortably will decrease substantially the uncertainties involved, and allow observed and model parameters to be matched iteratively.

Finally we also need an explanation for the two subsubgiant binaries observed in M67, S1063 and S1113. These lie below the base of the GB (BGB) in the CMD and to the right of the MS, much further displaced than the binary MS. S1063 has orbital parameters $P = 18.4\,\mathrm{d}$ and $e = 0.217$ while S1113 is circular with $P = 2.8\,\mathrm{d}$. HG stars respond to changes in mass on a thermal timescale (see Section 2.7 of Hurley, Pols & Tout 2000) so that as they lose mass they will evolve below the HG of the cluster isochrone. Mass transfer is consistent with the orbit of S1113 but not the eccentric orbit of S1063, unless the observed eccentricity could be for the outer orbit of a triple system. The population synthesis run PS6 produces 30 binaries in the subsubgiant area at 4.2 Gyr per 500 000 evolved. These are all circular, have a HG primary of average mass $1\,\mathrm{M}_\odot$, and an average period of 2 d. So if M67 originally had 15 000 binaries then one binary with these orbital parameters can be expected, i.e. S1113.

Possible evolution paths for S1063 are harder to find. The sub-luminous star may have formed in the same way as for S1113 and then been exchanged into an eccentric binary. However it is unlikely that two HG primaries are transferring mass at the same time and the exchange timescale for a short-period binary is long as has already been discussed. Another explanation is that a MS star with $M < M_{\mathrm{TO}}$ is evolving off the MS before it should. Consider a primordial binary with $M_1 = 1.4\,\mathrm{M}_\odot$, $M_2 = 0.4\,\mathrm{M}_\odot$, $P = 10\,\mathrm{d}$ and $e = 0.9$. At $T = 2\,500\,\mathrm{Myr}$ the more massive star begins to transfer mass to its companion. The normal MS lifetime of the primary is 3 370 Myr but due to the mass transfer it ages as it loses mass and at 2 700 Myr, when $M_1 = 1.2\,\mathrm{M}_\odot$, its effective MS lifetime is 4 200 Myr. If for some reason the mass transfer were halted at this point then the star would evolve off the MS at 4 200 Myr into the subsubgiant region. Exchange of the star into a wider binary is one way to halt the mass transfer and to explain the observed parameters of S1063. In run PS6 there are 600 likely exchange targets per 500 000 binaries but the window for exchange is small, as it must occur when $T_{\mathrm{MS}} \simeq 4\,200\,\mathrm{Myr}$, and so is the exchange cross-section. The exact nature of S1063 remains a mystery.

8 CONCLUSIONS

In order to complement increases in computing speed we have made a substantial effort to improve the treatment of physical processes within the cluster environment. Our N-body code includes detailed modelling of stellar and binary evolution, thus allowing us to test directly the influence of the interaction between stellar evolution and gravitational encounters on the evolution of a star cluster. Some similar advances have also been made in the work of Portegies Zwart et al (1998, 2000) although their models still only include Population I evolution and are therefore not suited to studying globular clusters. In particular, certain aspects of binary evolution, such as tidal circularization, are not modelled in as much detail as this work.

`NBODY4` is extremely useful for simulating cluster populations. As a first application we have modelled the blue straggler population in M67. We could just as easily have looked at many other aspects of cluster evolution, such as the production of CVs or development of mass segregation, but such topics will be the subject of future work. In particular, the availability of GRAPE-6 will enable us to model small globular clusters directly.

We have shown that binary evolution alone cannot account for the numbers of observed blue stragglers in open clusters, or the binary properties of these blue stragglers, when a realistic separation distribution is assumed. The influence of the cluster environment can effectively double the number of blue stragglers produced, leading to good agreement with the observations. Our N-body model of M67 demonstrates that blue stragglers are most likely generated by a variety of processes and in particular we find formation paths for all the BSs observed in M67. We also find that, among the possibilities we consider, the primordial binary population is best represented by a log-normal distribution of separations peaked at 10 AU and binary masses chosen from the mass function of Kroupa, Tout & Gilmore (1991) in combination with a uniform mass-ratio distribution.

We quantify the escape rate of stars from a cluster subject to the tidal field of our Galaxy as $\dot{M} = -0.3M/(t_{\mathrm{rh}} \log_{10} 0.4N)$. This enables us to provide a method by which the initial cluster mass and radius corresponding to current values can be determined. So we were able to model M67 by a semi-direct method even with current computational limitations.

ACKNOWLEDGMENTS

JRH thanks Trinity College and the Cambridge Commonwealth Trust for their generous support. CAT is very grateful to PPARC for support from an Advanced Fellowship. ORP thanks the Institute of Astronomy, Cambridge for supporting a number of visits undertaken during this work. We thank Douglas Heggie, Rainer Spurzem and Philipp Podsiadlowski for many helpful comments that improved the

quality of this manuscript. We also thank the referee (Mirek Giersz) for his suggestions on a number of important points.

REFERENCES

Aarseth S.J., 1963, MNRAS, 126, 223
Aarseth S.J., 1985, in Brackbill J.U., Cohen B.I., eds., Multiple Time Scales. Academic Press, New York, p. 377
Aarseth S.J., 1996, in Hut P., Makino J., eds., Dynamical Evolution of Star Clusters. IAU Symposium 174, Kluwer, Dordrecht, p.161
Aarseth S.J., 1999a, Celestial Mechanics and Dynamical Astronomy, 73, 127
Aarseth S.J., 1999b, PASP, 111, 1333
Aarseth S.J., Heggie D.C., 1998, MNRAS, 297, 794
Aarseth S., Hénon M., Wielen R., 1974, A&A, 37, 183
Aarseth S.J., Zare K., 1974, Celestial Mechanics, 10, 185
Abt H.A., 1983, ARA&A, 21, 343
Ahmad A., Cohen L., 1973, Journal of Computational Physics, 12, 389
Ahumada J., Lapasset E., 1995, A&AS, 109, 375
Bacon D., Sigurdsson S., Davies M.B., 1996, MNRAS, 281, 830
Baumgardt H., 1998, A&A, 330, 480
Belloni T., Verbunt F., Mathieu R.D., 1998, A&A, 339, 431 (BVM)
Binney J., Tremaine S., 1987, Galactic Dynamics. Princeton University Press, Princeton
Brandner W., Alcalá J.M., Kunkel M., Moreti A., Zinnecker H., 1996, A&A, 307, 121
Carraro G., Chiosi C., 1994, A&A, 288, 751
Carraro G., Chiosi C., Bressan A., Bertelli G., 1994, A&AS, 103, 375
Casertano S., Hut P., 1985, ApJ, 298, 80
Chernoff D.F., Weinberg M.D., 1990, ApJ, 351, 121
Davies M., 1996, in Hut P., Makino J., eds., Dynamical Evolution of Star Clusters. IAU Symposium 174, Kluwer, Dordrecht, p. 243
Duquennoy A., Mayor M., 1991, A&A, 248, 485
Eggleton P.P., Fitchett M., Tout C.A., 1989, ApJ, 347, 998 (EFT)
Elson R.A.W., Sigurdsson S., Davies M., Hurley J., Gilmore G., 1998, MNRAS, 300, 857
Fan X., Burstein D., Chen J.-S., Zhu J., Jiang Z., Wu H., Yan H., Zheng Z., Zhou X., Fang L.-Z., Chen F., Deng Z., Chu Y., Hester J.J., Windhorst A., Li Y., Lu P., Sun W.-H., Chen W.-P., Tsay W.-S., Chiueh T.-H., Chou C.-K., Ko C.-M., Lin T.-C., Guo H.-J., Byun Y.-I., 1996, AJ, 112, 628
Francic S.P., 1989, AJ, 98, 888
Friel E.D., Janes K.A., 1993, A&A, 267, 75
Giersz M., Heggie D.C., 1994, MNRAS, 268, 257
Giersz M., Heggie D.C., 1997, MNRAS, 286, 709
Girard T.M., Grundy W.M., López C.E., van Altena W.F., 1989, AJ, 98, 227
Goodman J., 1987, ApJ, 313, 576
Guhathakurta P., Webster T.Z., Yanny B., Schneider D.P., Bahcall J.N., 1998, AJ, 116, 1757
Hall D.S., 1976, in Fitch W.S., ed., Multiple Periodic Variable Stars. IAU Colloquim 29, Reidel, Dordrecht, p. 287
Heggie D.C., 1975, MNRAS, 173, 729
Heggie D.C., Aarseth S.J., 1992, MNRAS, 257, 513
Heggie D.C., Hut P., McMillan S.L.W., 1996, ApJ, 467, 359
Heggie D.C., Mathieu R.D., 1986, in Hut P., McMillan S.L.W., eds., The Use of Supercomputers in Stellar Dynamics. Springer-Verlag, Berlin, p. 233
Hobbs L.M., Thorburn J.A., 1991, AJ, 102, 1070
Hurley J.R., Aarseth S.J., Tout C.A., Gilmore G., Pols O.R., 2000, in ASP Conf. Ser. Vol. XXX, Star 2000: Dynamics of Star Clusters and the Milky Way, eds. S. Deiters, B. Fuchs, A. Just, R. Spurzem & R. Wielen (San Francisco: ASP), p. xxx
Hurley J.R., Pols O.R., Tout C.A., 2000, MNRAS, 315, 543
Hurley J.R., Tout C.A., 1998, MNRAS, 300, 977
Hurley J.R., Tout C.A., Pols O.R., 2000, MNRAS, submitted
Hut P., McMillan S., Goodman J., Mateo M., Phinney E.S., Pryor C., Richer H.B., Verbunt F., Weinberg M., 1992, PASP, 104, 981
Iben I.Jr., Livio M., 1993, PASP, 105, 1373
King I.R., 1966, AJ, 71, 64
Kippenhahn R., Weigert A., Hoffmeister R., 1967, in Alder B., Fernbach S., Rotenburg M., eds., Methods in Computational Physics, Vol. 7, Astrophysics, New York, p. 129
Kochanek C.S., 1992, ApJ, 385, 604
Kozai Y., 1962, AJ, 67, 591
Kroupa P., Tout C.A., Gilmore G., 1991, MNRAS, 251, 293
Kroupa P., Tout C.A., Gilmore G., 1993, MNRAS, 262, 545
Kustaanheimo P., Stiefel E., 1965, J. Reine Angew. Math., 218, 204
Kurucz R.L., 1992, in Barbuy B., Renzini A., eds., The Stellar Populations of Galaxies. IAU Symposium 149, Kluwer, Dordrecht, p. 225
Latham D.W., Milone A.A.E., 1996, in Milone E.F., Mermilliod J.-C., eds., The Origins, Evolution, and Destinies of Binary Stars in Clusters. ASP Conference Series 90, p. 385
Leonard P.J.T., 1996, ApJ, 470, 521
Leonard P.J.T., Linnell A.P., 1992, AJ, 103, 1928
Makino J., 1991, ApJ, 369, 200
Makino J., 1999, in Andersen J., ed., Highlights of Astronomy, Vol. 11B, as presented at the 23rd General Assembly of the IAU, 1997. Kluwer, Dordrecht, p. 597
Makino J., Kokubo E., Taiji M., 1993, PASJ, 45, 349
Mardling R.A., Aarseth S.J., 2000, MNRAS, submitted (MA)
Mathieu R.D., 1994, ARA&A, 32, 465
Mathieu R.D., Latham D.W., Griffin R., 1990, AJ, 100, 1859 (MLG)
Mathys G., 1991, A&A, 245, 467
McMillan S.L.W., 1986, in Hut P., McMillan S.L.W., eds., The Use of Supercomputers in Stellar Dynamics. Springer-Verlag, Berlin, p. 156
McMillan S.L.W., Hut P., Makino J., 1991, ApJ, 372, 111
Mermilliod J.-C., 1996, in Milone E.F., Mermilliod J.-C., eds., The Origins, Evolution, and Destinies of Binary Stars in Clusters. ASP Conference Series 90, p. 475
Meylan G., Heggie D., 1997, Astronomy & Astrophysics Review, 8, 1
Mikkola S., 1983, MNRAS, 203, 1107
Mikkola S., Aarseth S.J., 1990, Celestial Mechanics and Dynamical Astronomy, 47, 375
Mikkola S., Aarseth S.J., 1993, Celestial Mechanics and Dynamical Astronomy, 57, 439
Mikkola S., Aarseth S.J., 1998, New Astronomy, 3, 309
Miller R.H., 1964, ApJ, 140, 250
Milone A.A.E., Latham D.W., 1992a, in Kondo Y., Sistero R.F., Polidan R.S., eds., Evolutionary Processes in Interacting Binary Stars. IAU Symposium 151, Kluwer, Dordrecht, p. 473 (ML)
Milone A.A.E., Latham D.W., 1992b, in Kondo Y., Sisteró R.F., Polidan R.S., eds., Evolutionary Processes in Interacting Binary Stars. IAU Symposium 151, Kluwer, Dordrecht, p. 475
Montgomery K.A., Marschall L.A., Janes K.A., 1993, AJ, 106, 181 (MMJ)
Nissen P.E., Twarog B.A., Crawford D.L., 1987, AJ, 93, 634
Piotto G., Zoccali M., King I.R., Djorgovski S.G., Sosin C., Dorman B., Rich R.M., Meylan G., 1999, AJ, 117, 264
Press W.H., Teukolsky S.A., 1977, ApJ, 213, 183
Podsiadlowski P., 1996, MNRAS, 279, 1104
Pols O.R., Marinus M., 1994, A&A, 288, 475

Pols O.R., Schröder K.P., Hurley J.R., Tout C.A., Eggleton P.P., 1998, MNRAS, 298, 525
Popper D.M., 1980, ARA&A, 18, 115
Portegies Zwart S.F., Hut P., Makino J., McMillan S.L.W., 1998, A&A, 337, 363
Portegies Zwart S.F., Hut P., McMillan S.L.W., Verbunt F., 1997, A&A, 328, 143
Portegies Zwart S.F., McMillan S.L.W., Hut P., Makino J., 2000, MNRAS, submitted
Quinlan G.D., Tremaine S., 1992, MNRAS, 259, 505
Rasio F.A., Heggie D.C., 1995, ApJ, 445, L133
Richer H.B., Fahlman G.G., Ibata R.A., Pryor C., Bell R.A., Bolte M., Bond H.E., Harris W.E., Hesser J.E., Holland S., Ivanans N., Mandushev G., Stetson P.B., Wood M.A., 1997, ApJ, 484, 741
Richer H.B., Fahlman G.G., Rosvick J., Ibata R., 1998, ApJ, 116, L91
Sanders W.L., 1977, A&AS, 27, 89
Simon M., Ghez A.M., Leinert Ch., Cassar L., Chen W.P., Howell R.R., Jameson R.F., Matthews K., Neugebauer G., Richichi A., 1995, ApJ, 443, 625
Spitzer L.Jr., 1987, Dynamical Evolution of Globular Clusters. Princeton University Press, Princeton
Tout C.A., Aarseth S.J., Pols O.R., Eggleton P.P., 1997, MNRAS, 291, 732
Tout C.A., Eggleton P.P., 1988, MNRAS, 231, 823
Tout C.A., Kembhavi A., 1993, in Smith G.H., Brodie J.P., eds., The globular clusters-galaxy connection. ASP Conference Series 48, p. 226
Terlevich E., 1987, MNRAS, 224, 193
van den Berg M., Verbunt F., Mathieu R.D., 1999, A&A, 347, 866 (MVB)
Webbink R.F., 1988, in Mikolajewska J., Friedjung M., Kenyon S.J., Viotto R., eds., The Symbiotic Phenomenon. IAU Colloquim 103, Kluwer, Dordrecht, p. 311
Wilkinson M.I., Evans N.W., 1999, MNRAS, 310, 645
Wilkinson M.I., Hurley J.R, 2001, in preparation
Zare K., 1977, Celestial Mechanics, 16, 35